ARCHIVES OF ACOUSTICS
24, 3, 331–364 (1999)

ULTRASONIC TRANSDUCER FOR THE RECEPTION OF ACOUSTIC EMISSION SIGNALS OF THE TEMPOROMANDIBULAR JOINT

R. SALAMON, W. LIS

Department of Acoustics
Technical University of Gdańsk
(80-052 Gdańsk, ul. G. Narutowicza 11/12, Poland)
e-mail: wall@eti.pg.gda.pl

J. ZIENKIEWICZ

Department and Clinic of Maxillofacial Surgery
Medical Academy in Gdańsk
(ul. Dębinki 7, Poland)

Auscultation and analysis of acoustic signals emitted by the human body are widely used in medical diagnosing. Acoustic signals are also emitted by joints, including the temporomandibular joint, which is the subject of this paper. A system was developed to receive, record, process and display the signals emitted by this particular joint. The article presents an essential fragment of the system, namely a special ultrasonic transducer designed to receive acoustic signals emitted by the temporomandibular joint. At first, the particular requirements were established in the area of the parameters and functions of the transducer. Following that, a technological solution was proposed. Next, a model of the transducer was analysed using the difference equation method with continuous time. The solution of these equations is the pulse response of the transducer and in the frequency domain, it is the shift function. These functions were used for an in-depth analysis of the effects of the transducer's construction on its parameters and values. Based on these findings, a methodology of the design of the transducer was developed. The transducer was designed and built according to the methodology. It was subsequently studied in detail. The results of the study have confirmed that the method of the analysis and the design were correct. Finally, the article presents some examples of real signals of acoustic emission of the temporomandibular joint as they were received by the ultrasonic transducer built in the course of the work.

1. Introduction

As we know, the human system is a source of numerous acoustic signals among which the speech signal is the most important and best-researched one. These signals are generated by the movements of muscles and joints and by the flow of blood and air. Since long ago auscultation of the signals made by the human body has been one of

medicine's basic methods of diagnosing. Usually a diagnosis is made based on a subjective assessment of the acoustic signal with the credibility of the diagnosis largely depending on the experience and predisposition of the doctor. This method of using acoustic signals proves successful in the diagnosis of lungs and heart diseases but is of little use in the diagnosis of muscles and joints. Acoustic signals that are emitted by muscles and joints usually feature an uncomplicated course and are not intense enough for an auscultation with a phonendoscope to be efficient. Additionally, the phonendoscope method does not allow for a signal recording and further analysis, which consequently makes the diagnosis' objectivity impossible.

One of the joints that deserves special attention is the temporomandibular joint which when diseased causes severe impairment of man's important functions such as speaking, eating and facial expression. The acoustic emission evoked by the movement of this joint, can be easily observed especially by the person setting the mandible in motion. Signals generated by the joint can also be heard using a phonendoscope. This was observed and used in the studies of the occlusion by D. WATT already in the sixties, [20]. First attempts to record the signals emitted by the temporomandibular joint were made in the seventies by, among others, YOWELOW [22] and J. and Z. KRASZEWSCY [9–10]. They would use a microphone to receive acoustic signals and a tape recorder or an electrocardiograph to record them. In the following years the technique of signal recording was improved as were the methods of processing these signals, [1–4, 6, 7, 11, 12, 16, 21]. A general and important result of these and later studies is the estimation of the width of the spectrum of acoustic emission signals. It matches the band of audiofrequencies. When, however, the frequency is more than several kilohertz the spectrum level quickly drops and reaches the level of noise. The least attention was given to the electroacoustic transducer even though its parameters largely determine the quality of the whole diagnostic apparatus. The authors are unaware of any reports in the literature on the optimisation of the construction of transducers in terms of adjusting their parameters to the specific requirements of reception of acoustic signals emitted by the temporomandibular joint. The article presents the results of a theoretical analysis, the construction and results of studies on a special transducer built to record and process acoustic emission signals made by the temporomandibular joint.

2. Mathematical model of the transducer receiving acoustic emission signals made by the temporomandibular joint

Studies on acoustic emission of the temporomandibular joint made so far used various types of microphones or less often accelerometers as electroacoustic transducers. Since the structure of all microphones is made to receive acoustic waves in the air, there is a concern whether the microphone is the appropriate device to measure waves propagated within the human body, especially those observed in the soft tissues surrounding the joint itself and the adjacent bone structure. The reason for this concern is that the acoustic properties of air and tissues are completely different which is expressed, among other things, by the big difference in acoustic impedance of both media. Acoustic impedance of

soft tissues is 5000 times greater than the impedance of air. Consequently, microphones operating in the air are activated by acoustic waves with high deflections and small pressures whereas when used in soft tissues they are activated by waves of high pressures and small deflections. Therefore, what we are dealing here with is a situation that is more typical for ultrasonic medical diagnosis or hydroacoustics rather than for audioacoustics. In both fields piezoceramic transducers are used commonly both for transmission and reception of acoustic waves.

To obtain better results than those produced by microphones one should turn to broadband ultrasonic transducers. Transducers like these are made as piezoceramic transducers with matching layers [15], as composite transducers [14] and accelerometers [17]. The first two types of transducers have a broad transmitted frequency band, however, it is located around a certain relatively high mid-band frequency. Therefore, it does not include very low audio-frequencies, which are included in the spectrum of acoustic emission signals of the temporomandibular joint. Accelerometers are used commonly in measurements of mechanical vibrations and their band covers the desired range of frequencies. However, the medium that the accelerometer is in contact with is usually a solid body whose characteristic acoustic impedance is greater than the soft tissue impedance, however, the disproportion in this case is not as big as between the tissues and air. Despite that, direct attempts to use standard accelerometers to receive acoustic emission signals coming from a patient's body are not without a doubt. The vibrations of the accelerometer are usually enforced by the vibrations of a big mass (e.g. the steel body of a machine or vehicle). Because of the significantly smaller mass and geometric dimensions of the accelerometer, it does not affect the distribution of vibrations of the measured object and the whole object-accelerometer system does not have to be seen in wave terms. This simplification is not justified when the accelerometer is in contact with a soft tissue where the acoustic wave propagates similarly to its propagation in liquids. Nonetheless, the very idea of using a piezoelectric transducer that constitutes an active element of the accelerometer and the use of a big mass to weight it on the back side seems to deserve a thorough analysis.

Following the above notions, a system was selected to act as a simplified theoretical model of an electroacoustic transducer. The system consisted of a piezoceramic transducer in the shape of an extended rectangular prism with a metal cylinder as its weighting placed on the back surface. It was assumed that the activation would originate from a plane acoustic wave, which propagates in a liquid inorganic medium and is perpendicular to the front surface of the piezoceramic transducer. The electrical signal is observed on electrodes attached to the front and back surface of the piezoceramic transducer. The piezoceramic transducer is polarised perpendicularly to the electrodes. Figure 1 shows a simplified form of the transducer.

At the output of the transducer the electrical signal in question can be determined using numerical methods (e.g. the finite elements methods) or analytical methods. Since the objective is not to analyse a singular case but to define some general relations, which could describe the operations of the transducer, in this case we decided to use the analytical method. The principles of this method were developed for designing broadband transducers with matching layers [15, 17–19].

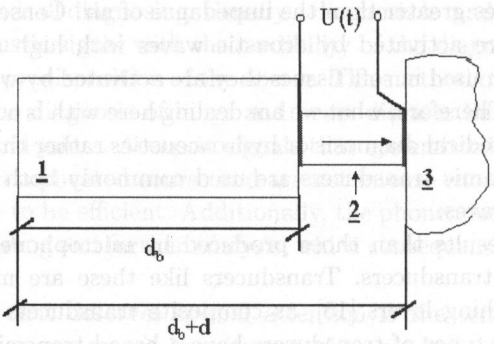

Fig. 1. A simplified form of the transducer receiving acoustic emission signals.

Let us assume that in a piezoceramic transducer and in the metal cylinder only the plane acoustic wave propagates perpendicularly to the electrodes. Let us also assume that mechanical and electrical loss in both elements is negligibly small and that the back surface of the metal cylinder is weighted with an unlimited medium — the air. Given such assumptions the vibrations of the whole system can be described using the velocities shown in Fig. 2.

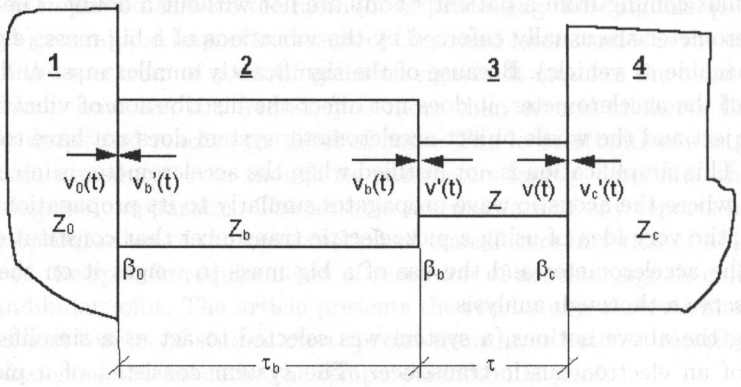

Fig. 2. Physical model of the transducer.

The symbols seen in the figure have the following physical interpretation:

• acoustic velocities $v_o(t)$, $v_b(t)$, $v_b'(t)$, $v(t)$, $v'(t)$ and $v_c'(t)$ are courses of component velocities of waves that are incident to the boundaries of the media,

• delays $\tau = d/c$ and $\tau_b = d_b/c_b$ are the duration of propagation of the longitudinal acoustic wave respectively between the electrodes of the piezoceramic plate and base of the metal cylinder (d — length of the piezorceramic transducer, c — velocity of the longitudinal wave in the piezoceramic transducer, d_b — length of the metal cylinder, c_b — velocity of the longitudinal wave in the metal cylinder),

• reflection coefficients β_0, β_c, and β_b, are mechanical coefficients of reflection on the boundaries of the respective media, defined for the forces ($\beta_0 = (Z_b - Z_0)/(Z_b + Z_0)$, $\beta_b = (Z - Z_b)/(Z + Z_b)$, $\beta_c = (Z_c - Z)/(Z_c + Z)$, where $Z_b = A_b\rho_b c_b$ is the mecha-

nical impedance of the base of the metal cylinder with surface A_b, density volume ρ_b and velocity of the longitudinal acoustic wave c_b, $Z_0 = A_b\rho_0 c_0$ which is the mechanical impedance of the medium on the left side of the cylinder's base, $Z = A\rho c$ is the mechanical impedance of the transducer and $Z_c = A_c\rho_c c_c$ is the mechanical impedance of tissues).

Our task is to determine the voltage $U(t)$ on open electrodes of the piezoceramic transducer as a function of acoustic velocity $v_c'(t)$ of a wave which is incident perpendicularly to the surface of the transducer from the direction of the tissues. If we assume that the shape of the transducer is close to that of a thin rod, voltage $U(t)$ can be described using the following relation, [5, 8]:

$$U(t) = Y_3^D g_{33} \int_0^t [V_b(t) - V_c(t)]\, dt, \tag{1}$$

where Y_3^D is the Young's modulus elasticity given a constant induction D, and g_{33} — a piezoelectric constant, and $V_b(t)$ and $V_c(t)$ the velocities of vibrations of the back and front surface of the piezoelectric transducer respectively.

The velocities of vibrations of the surfaces $V_c(t)$ and $V_b(t)$ are the sums of acoustic waves that are incident to, reflected from and going across the boundaries of the medium on the left or right side of the boundary. They can be easily determined using Fig. 2 and the functional diagram of the wave system in question as shown in Fig. 3.

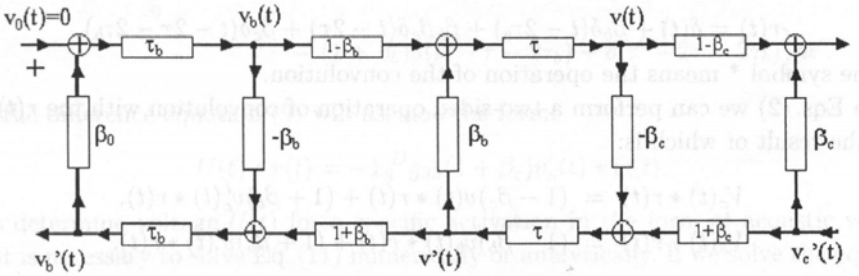

Fig. 3. Functional diagram of the transducer.

They are described with the following relations:

$$\begin{aligned} V_c(t) &= (1-\beta_c)v(t) + (1+\beta_c)v_c'(t), \\ V_b(t) &= (1-\beta_b)v_b(t) + (1+\beta_b)v'(t). \end{aligned} \tag{2}$$

As you can see, to calculate the velocity of vibrations of the transducer's surface it is necessary to know the velocity components $v(t)$, $v_b(t)$, $v'(t)$. These velocities can be determined using the below system of equations put together on the basis of the functional diagram from Fig. 3.

$$\begin{aligned} v_b(t) &= (1-\beta_0)v_o(t-\tau_b) + \beta_0 v_b'(t-\tau_b), \\ v_b'(t) &= (1+\beta_b)v'(t-\tau_b) - \beta_b v_b(t-\tau_b), \\ v(t) &= (1-\beta_b)v_b(t-\tau) + \beta_b v'(t-\tau), \\ v'(t) &= (1+\beta_c)v_c'(t-\tau) - \beta_c v(t-\tau). \end{aligned} \tag{3}$$

To solve this system of equations, first we need to notice that the characteristic acoustic impedance of the base of the metal cylinder is much bigger than the acoustic impedance of air. This makes the reflection coefficient β_0 practically equal to one. The equations (3) are then simplified to obtain the form of:

$$\begin{aligned} v_b(t) &= v_b'(t-\tau_b), \\ v_b'(t) &= (1+\beta_b)v'(t-\tau_b) - \beta_b v_b(t-\tau_b), \\ v(t) &= (1-\beta_b)v_b(t-\tau) + \beta_b v'(t-\tau), \\ v'(t) &= (1+\beta_c)v_c'(t-\tau) - \beta_c v(t-\tau). \end{aligned} \tag{4}$$

The above equations contain four unknown functions; they are $v_b(t)$, $v_b'(t)$, $v(t)$, $v'(t)$. Function $v_c'(t)$ is the activation that we know from the assumption. This means that this system of equations can be solved and each of the velocities that we are looking for can be determined as a function of activation. The solution to this untypical system of equations is given in the Appendix. Below we are presenting the result of the solution only:

$$\begin{aligned} v_b(t) * r(t) &= (1+\beta_b)(1+\beta_c)v_c'(t-\tau-2\tau_b), \\ v'(t) * r(t) &= (1+\beta_c)\left[v_c'(t-\tau) + \beta_b v_c'(t-\tau-2\tau_b)\right], \\ v(t) * r(t) &= (1+\beta_c)\left[v_c'(t-2\tau-2\tau_b) + \beta_b v_c'(t-2\tau)\right]. \end{aligned} \tag{5}$$

where

$$r(t) = \delta(t) + \beta_b\delta(t-2\tau_b) + \beta_b\beta_c\delta(t-2\tau) + \beta_c\delta(t-2\tau-2\tau_b), \tag{6}$$

and the symbol * means the operation of the convolution.

On Eqs. (2) we can perform a two-sided operation of convolution with the $r(t)$ function, the result of which is:

$$\begin{aligned} V_c(t) * r(t) &= (1-\beta_c)v(t) * r(t) + (1+\beta_c)v_c'(t) * r(t), \\ V_b(t) * r(t) &= (1-\beta_b)v_b(t) * r(t) + (1+\beta_b)v'(t) * r(t). \end{aligned} \tag{7}$$

On the right-hand side of Eqs. (7) there are convolutions of the velocities with the $r(t)$ function which we can see on the left-hand side of the equations, too (5). Therefore, we can make the appropriate substitutions as a result of which we get:

$$\begin{aligned} V_c(t) * r(t) &= (1+\beta_c)\left[v_c'(t-2\tau-2\tau_b) + \beta_b v_c'(t-2\tau)\right] + v_c'(t) + \beta_b v_c'(t-2\tau_b), \\ V_b(t) * r(t) &= (1+\beta_b)(1+\beta_c)\left[v_c'(t-\tau-2\tau_b) + v_c'(t-\tau)\right]. \end{aligned} \tag{8}$$

The equation we have been looking for which contains only activation $v_c'(t)$ and response in the form of voltage $U(t)$ is obtained by performing on Eq. (1) the operation of convolution with the $r(t)$ function and by substituting Eqs. (8). As a result, we get:

$$\begin{aligned} U(t) * r(t) = -Y_3^D g_{33}(1+\beta_c)v_c'(t) * \int_0^t \Big[&\delta(t') - (1+\beta_b)\delta(t'-\tau) + \beta_b\delta(t'-2\tau) \\ &+ \beta_b\delta(t'-2\tau_b) - (1+\beta_b)\delta(t'-\tau-2\tau_b) + \delta(t'-2\tau-2\tau_b)\Big]dt'. \end{aligned} \tag{9}$$

In this way the voltage in question $U(t)$ has been described using a *non-homogenous difference equation* with a continuous duration in which on the left-hand side is a convolution of voltage $U(t)$ with function $r(t)$, and on the right-hand side a convolution of activation $v_c'(t)$ with a function written down in the above equation as an integral. Equation (9) can be treated as a mathematical model of the transducer. It can be used to analyse it in the time domain and also — after the necessary transformations — to analyse it in the frequency domain.

3. Analysis in the time domain

Analysis in the time domain is usually used to determine the response of a linear system to specific activation we are investigating. This method is less frequently used to research the general properties of a system. To that end the analysis in the frequency domain gives more insight and is therefore more frequently used. Nonetheless from the theoretical standpoint both methods are equivalent and will be presented below.

To simplify the notation of the equations let us mark the integral expression in Eq. (9) as:

$$w(t) = \int_0^t \Big[\delta(t') - (1+\beta_b)\delta(t'-\tau) + \beta_b\delta(t'-2\tau) + \beta_b\delta(t'-2\tau_b) - (1+\beta_b)\delta(t'-\tau-2\tau_b) + \delta(t'-2\tau-2\tau_b)\Big]dt'. \tag{10}$$

Then the difference equation (9) will assume the form:

$$U(t) * r(t) = -Y_3^D g_{33}(1+\beta_c)v_c'(t) * w(t). \tag{11}$$

To determine voltage $U(t)$ for a specific activation in the form of acoustic velocity $v_c'(t)$ it is necessary to solve Eq. (11) numerically or analytically. If we solve the equation directly, then for each activation we have to repeat all calculations, which are not always simple. This inconvenience can be eliminated by using *pulse responses*. To that end, let us introduce the term of a *homogenous difference equation* of the considered system. It can be noted as:

$$k(t) * r(t) = \delta(t), \tag{12}$$

or in the full form as:

$$k(t) + \beta_b k(t-2\tau_b) + \beta_b\beta_c k(t-2\tau) + \beta_c k(t-2\tau-2\tau_b) = \delta(t), \tag{13}$$

where $\delta(t)$ is Dirac's function, and $k(t)$ — *pulse response of a homogenous equation.*

Now let us write the difference equation (11) as a convolution with pulse response $k(t)$:

$$U(t) * r(t) * k(t) = -Y_3^D g_{33}(1+\beta_c)v_c'(t) * w(t) * k(t). \tag{14}$$

Using Eq. (12), we get:

$$U(t) = -Y_3^D g_{33}(1+\beta_c)v_c'(t) * w(t) * k(t). \tag{15}$$

As you can see, voltage $U(t)$ can be calculated as a convolution of activation $v_c'(t)$ with pulse response $k(t)$ and function $w(t)$. The saving in the computation is that both pulse response $k(t)$ and function $w(t)$ are dependent solely on the parameters of the analysed system. Therefore, they can be computed once and then used multiple times to determine response $U(t)$ to random activation $v_c'(t)$.

Pulse response $k_u(t)$ of the analysed system according to the theory of linear systems is equal to the system's response to activation in the form of Dirac's pulse. That's why by adding $v_c'(t) = \delta(t)$ to Eq. (15) we get:

$$k_u(t) = -Y_3^D g_{33}(1 + \beta_c)w(t) * k(t) \tag{16}$$

and

$$U(t) = k_u(t) * v_c'(t). \tag{17}$$

The result of the transformations we have applied is the following procedure of determining the voltage on open electrodes of the sensor's piezoceramic plate:

- by solving the homogenous difference equation (12) we determine the $k(t)$ pulse response,
- we determine the $w(t)$ function from relation (10),
- from Eq. (16) we calculate pulse response $k_u(t)$,
- we calculate voltage $U(t)$ as a convolution of activation $v_c'(t)$ with pulse response $k_u(t)$ (Eq. (17)).

The only, slightly less frequent mathematical problem that is present in this computational method is the solution of the difference equation with a continuous time

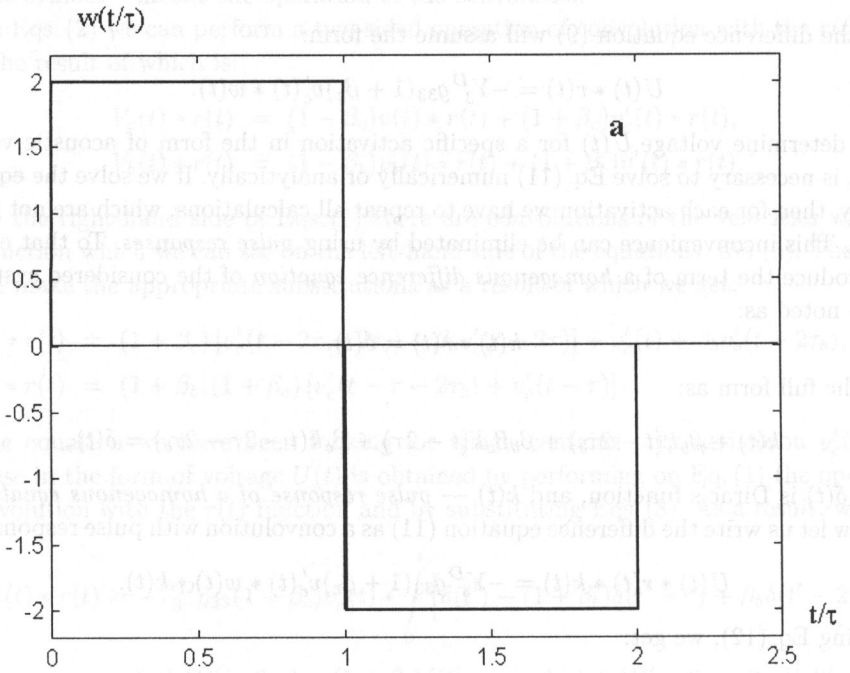

[FIG. 4a]

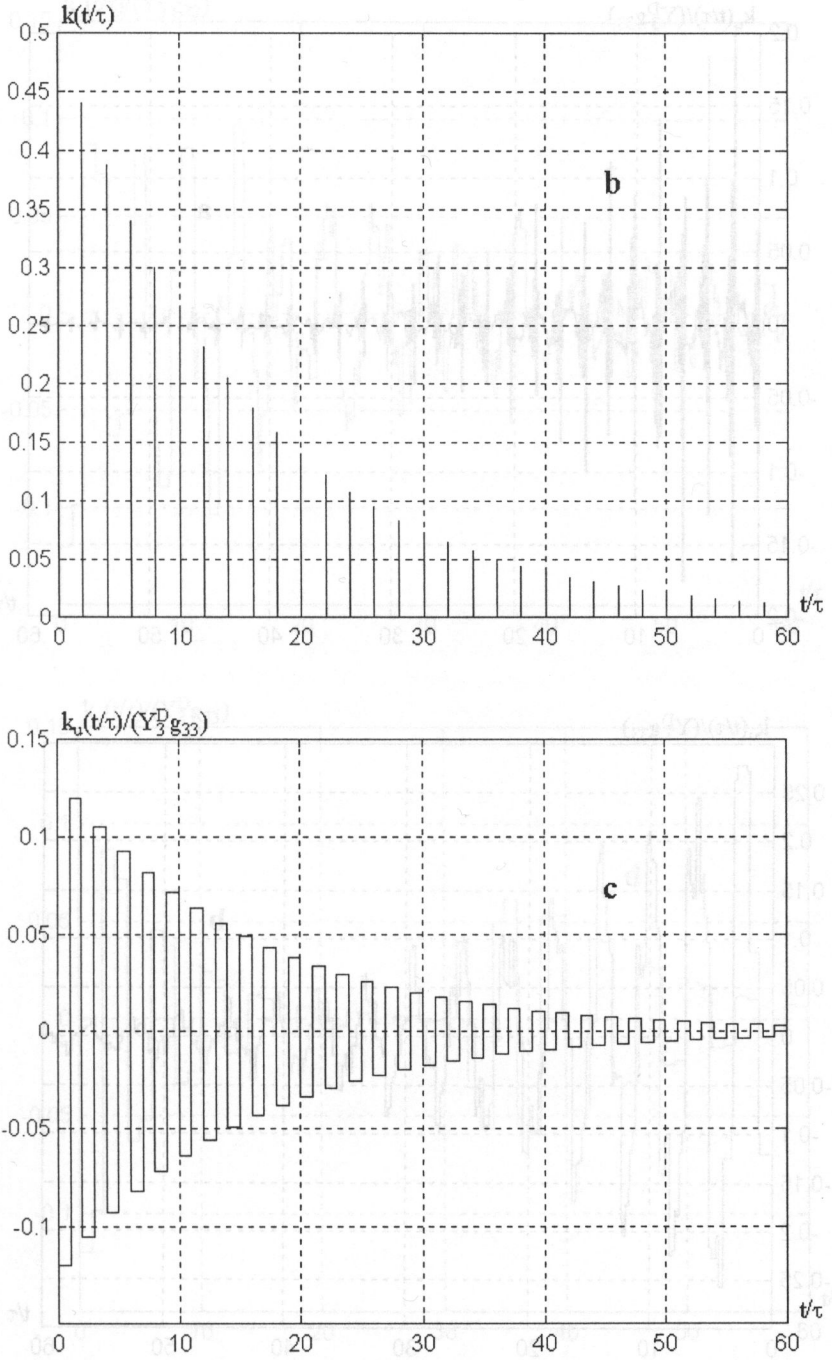

Fig. 4. The forming of the transducer's pulse response without the metal cylinder ($\beta_b = 1$, $\beta_c = -0.88$): a) function $w(t)$, b) auxiliary function $k(t)$, c) pulse response of the transducer.

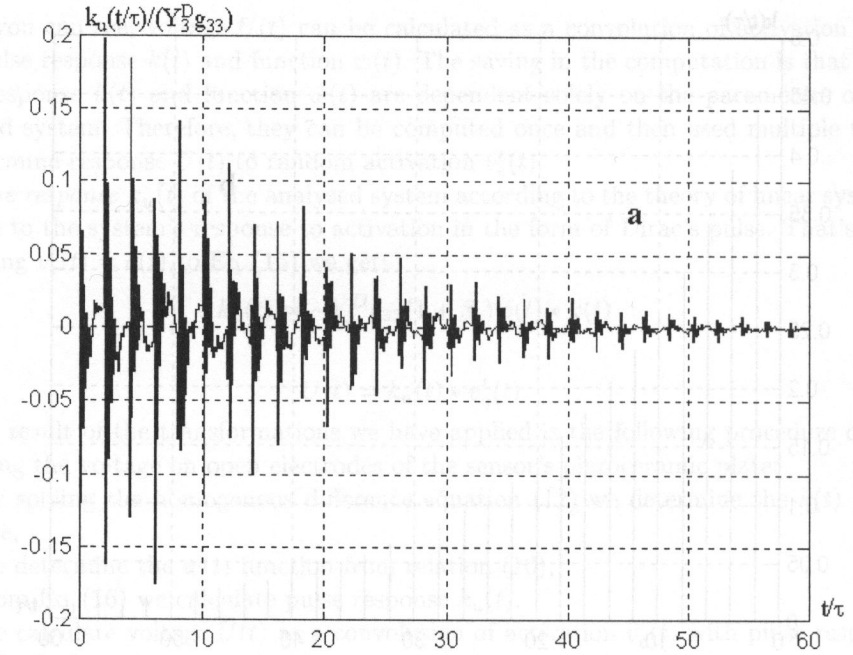
$k_u(t/\tau)/(Y_3^D g_{33})$
0.2
0.15
0.1
0.05
0
-0.05
-0.1
-0.15
-0.2
0
10
20
30
40
50
60
t/τ
a

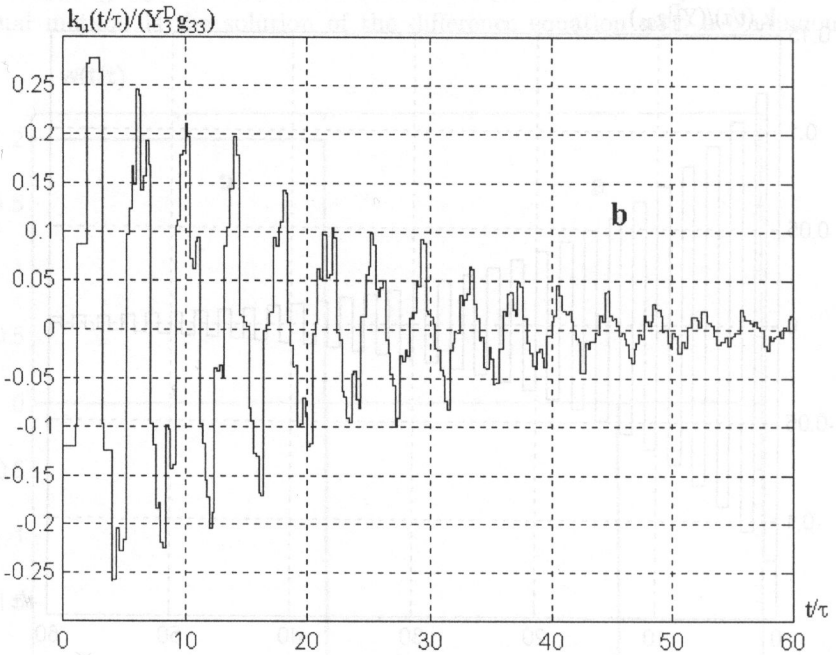
$k_u(t/\tau)/(Y_3^D g_{33})$
0.25
0.2
0.15
0.1
0.05
0
-0.05
-0.1
-0.15
-0.2
-0.25
0
10
20
30
40
50
60
t/τ
b

[FIG. 5 a, b]

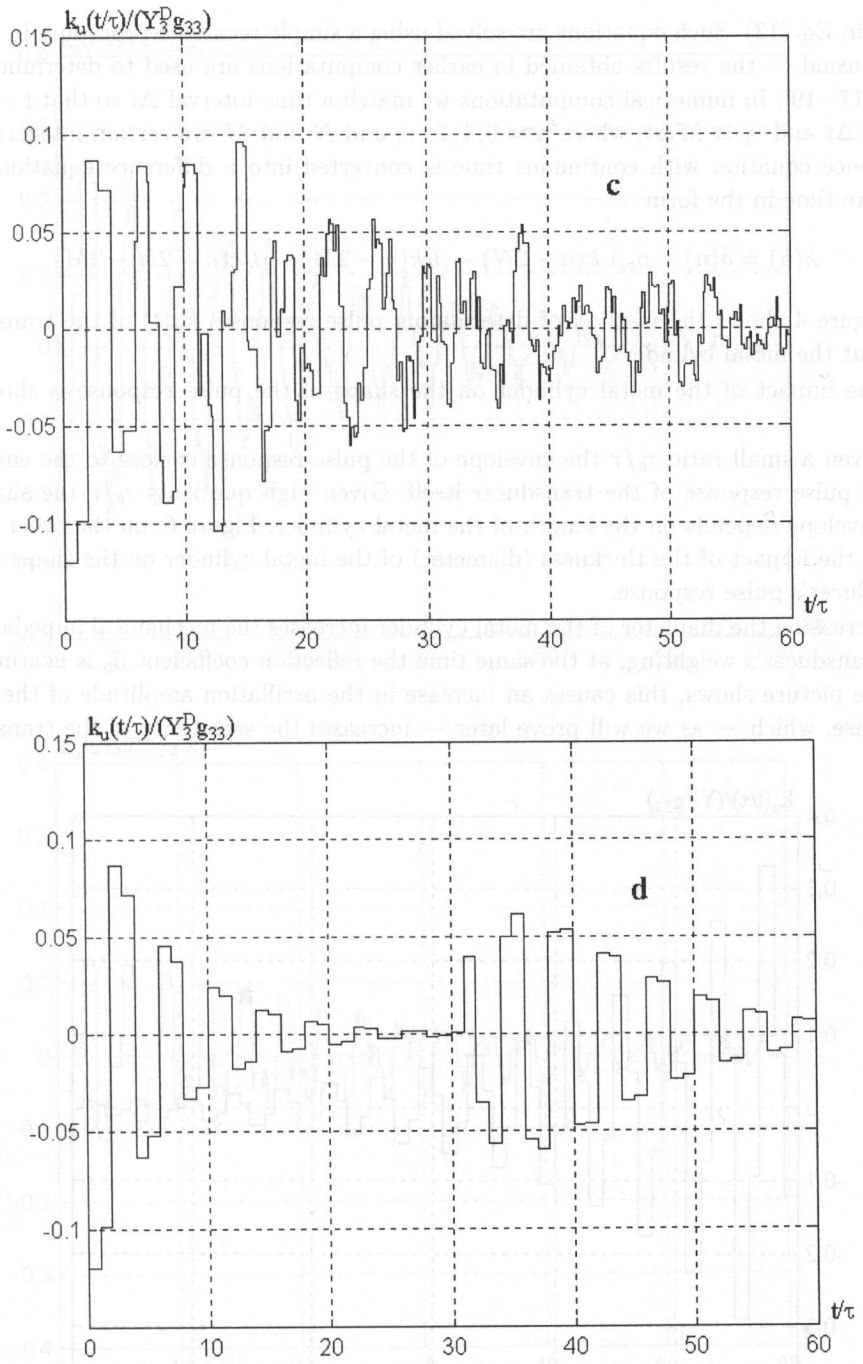

Fig. 5. The effects of the length of the metal cylinder on the pulse response of the transducer ($\beta_b = -0.823$, $\beta_c = -0.88$): a) $\tau_b/\tau = 0.05$, b) $\tau_b/\tau = 0.6$, c) $\tau_b/\tau = 2.6$, d) $\tau_b/\tau = 15$.

given in Eq. (13). Such equations are solved using a simple recurrent procedure in which — as usual — the results obtained in earlier computations are used to determine new ones [17–19]. In numerical computations we match a time interval Δt so that $t = n\Delta t$, $\tau \cong N\Delta t$ and $\tau_b \cong M\Delta t$, where $n = 0, 1, 2, ...$, and N and M are certain integers. The difference equation with continuous time is converted into a difference equation with discrete time in the form of:

$$k(n) = \delta(n) - \beta_b\beta_c k(n - 2N) - \beta_b k(n - 2M) - \beta_c k(n - 2N - 2M). \tag{18}$$

Figure 4 shows the method of determining pulse responses $k_u(t)$ of the transducer without the metal cylinder.

The impact of the metal cylinder on the shape of the pulse response is shown in Fig. 5.

Given a small ratio τ_b/τ the envelope of the pulse response is close to the envelope of the pulse response of the transducer itself. Given high quotients τ_b/τ the shape of the envelope depends on the length of the metal cylinder. Figure 6, on the other hand, shows the impact of the thickness (diameter) of the metal cylinder on the shape of the transducer's pulse response.

Increasing the diameter of the metal cylinder increases the mechanical impedance of the transducer's weighting, at the same time the reflection coefficient β_b is nearing -1. As the picture shows, this causes an increase in the oscillation amplitude of the pulse response, which — as we will prove later — increases the sensitivity of the transducer

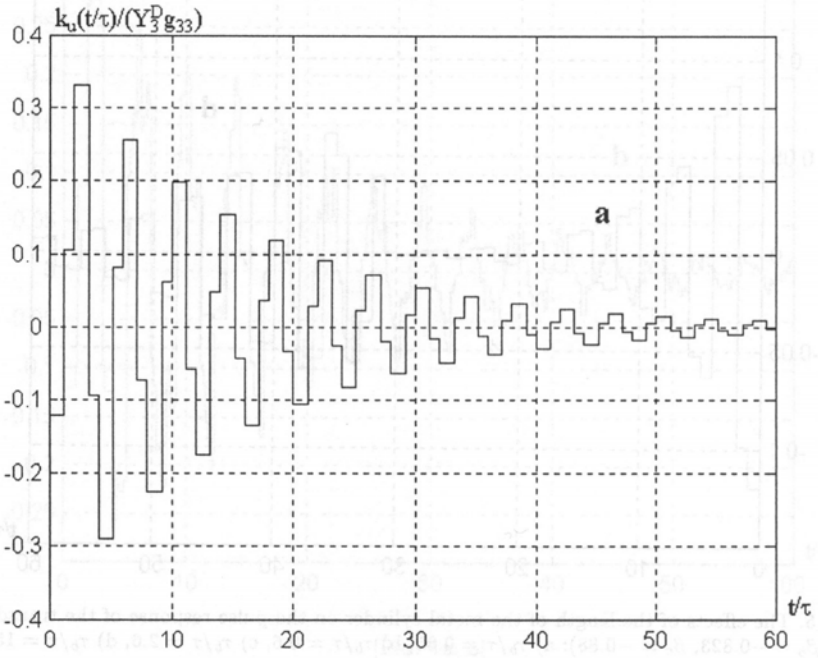

[FIG. 6 a]

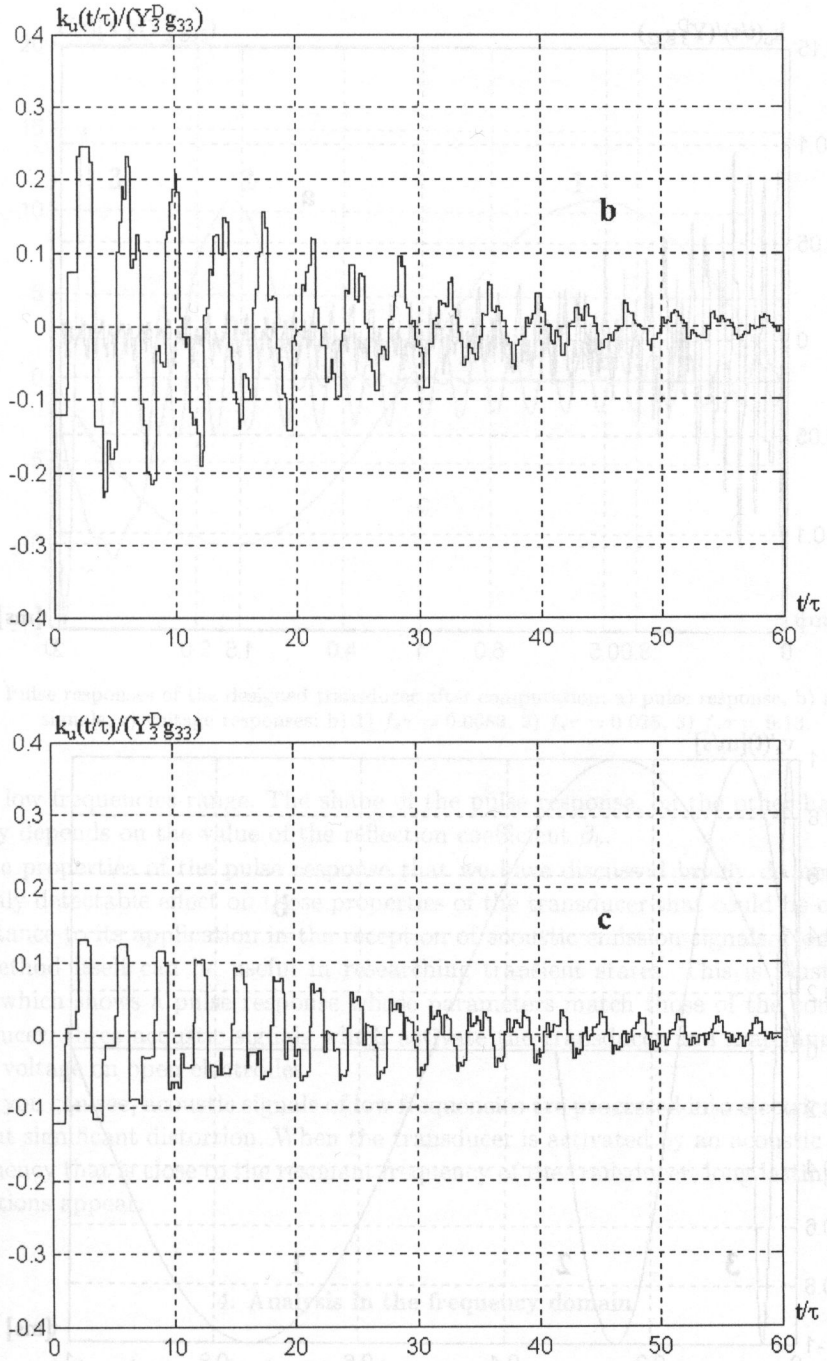

Fig. 6. The effects of the diameter of the metal cylinder on the pulse response of the transducer ($\tau_b/\tau = 0.6$, $\beta_c = -0.88$): a) $\beta_b = -1$, b) $\beta_b = -0.7$, c) $\beta_b = -0.1$.

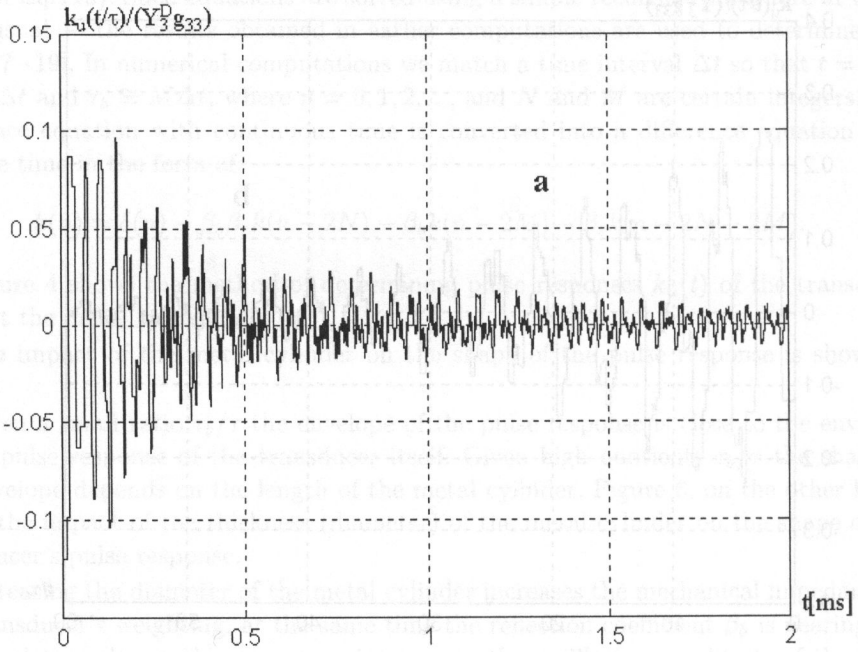
$k_a(t/\tau)/(Y_3^D g_{33})$
0.15
0.1
0.05
0
-0.05
-0.1
a
0
0.5
1
1.5
2
t[ms]

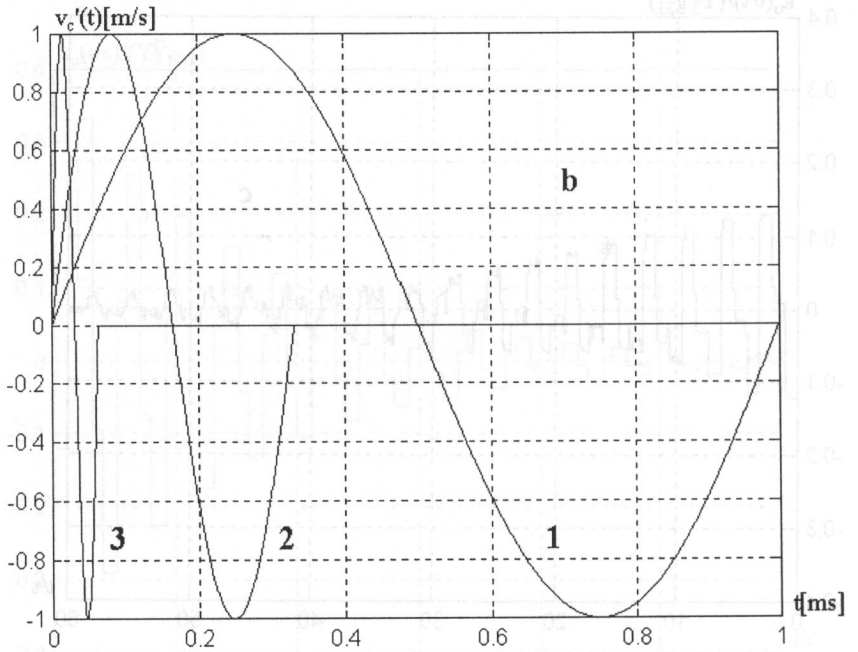
$v_c'(t)$[m/s]
1
0.8
0.6
0.4
0.2
0
-0.2
-0.4
-0.6
-0.8
-1
b
3
2
1
0
0.2
0.4
0.6
0.8
1
t[ms]

[FIG. 7 a, b]

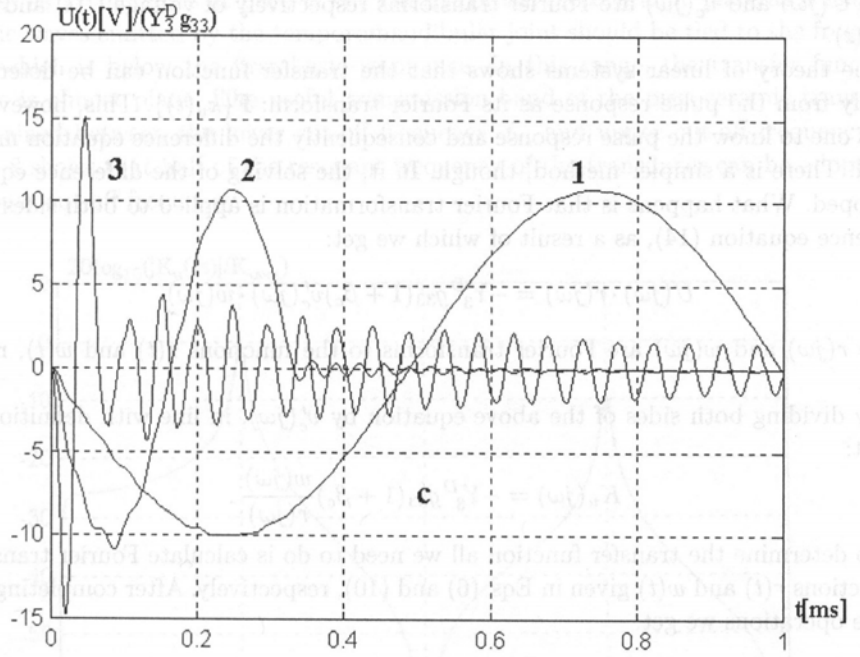

Fig. 7. Pulse responses of the designed transducer after computation: a) pulse response, b) activating signals, c) voltage responses: b) 1) $f_s\tau = 0.0083$, 2) $f_s\tau = 0.025$, 3) $f_s\tau = 0.13$.

in the low frequencies range. The shape of the pulse response, on the other hand, only slightly depends on the value of the reflection coefficient β_b.

The properties of the pulse response that we have discussed briefly do not exhibit an easily detectable effect on those properties of the transducer that could be of critical importance to its application in the reception of acoustic emission signals. Nonetheless, the method itself can be useful in researching transient states. This is illustrated in Fig. 7 which shows a pulse response whose parameters match those of the constructed transducer, three acoustic signals which activate the transducer and matching courses of the voltage on open electrodes.

As you can see, acoustic signals of low frequencies are processed into electrical signals without significant distortion. When the transducer is activated by an acoustic signal of a frequency that is close to the resonant frequency of the transducer, long lasting voltage oscillations appear.

4. Analysis in the frequency domain

Let us define the transfer function of the transducer as:

$$K_u(j\omega) = \frac{U(j\omega)}{v_c'(j\omega)}, \tag{19}$$

where $U(j\omega)$ and $v_c'(j\omega)$ are Fourier transforms respectively of voltage $U(t)$ and velocity $v_c'(t)$.

The theory of linear systems shows that the transfer function can be determined directly from the pulse response as its Fourier transform: $\mathbf{F}\{k_u(t)\}$. This, however, requires one to know the pulse response and consequently the difference equation must be solved. There is a simpler method, though. In it, the solving of the difference equation is skipped. What happens is that Fourier transformation is applied to both sides of the difference equation (14), as a result of which we get:

$$U(j\omega)\cdot r(j\omega) = -Y_3^D g_{33}(1+\beta_c)v_c'(j\omega)\cdot w(j\omega), \tag{20}$$

where $r(j\omega)$ and $w(j\omega)$ are Fourier transforms to the functions $r(t)$ and $w(t)$, respectively.

By dividing both sides of the above equation by $v_c'(j\omega)$, in line with definition (19) we get:

$$K_u(j\omega) = -Y_3^D g_{33}(1+\beta_c)\frac{w(j\omega)}{r(j\omega)}. \tag{21}$$

To determine the transfer function all we need to do is calculate Fourier transforms of functions $r(t)$ and $w(t)$ given in Eqs. (6) and (10), respectively. After completing these simple operations we get:

$$K_u(j\omega) = j\frac{Y_3^D g_{33}(1+\beta_c)}{\omega} \cdot \frac{1-(1+\beta_b)e^{-j\omega\tau}+\beta_b e^{-j2\omega\tau}+\left[\beta_b-(1+\beta_b)e^{-j\omega t}+e^{-j2\omega\tau}\right]e^{-j2\omega\tau_b}}{1+\beta_b e^{-j2\omega\tau_b}+\beta_b\beta_c e^{-j2\omega(\tau+\tau_b)}}. \tag{22}$$

Using the above formula, we can study the effects of the particular parameters of the transducer on the course of its transfer function. We will begin this study by determining the transfer function of the piezoceramic transducer weighted with air from the backside. It will be a good model for defining the effects of the parameters of the metal cylinder on the performance of the whole transducer. To that end we add to Eq. (22) $\beta_b = 1$ and get:

$$K_u(i\omega) = j\frac{Y_3^D g_{33}(1+\beta_c)}{\omega}\cdot\frac{1-2e^{-j\omega\tau}+e^{-j2\omega\tau}}{1+\beta_c e^{-j2\omega\tau}}. \tag{23}$$

Figure 8 shows a module of the transfer function described with formula (23). On the X-axis the scale $f\tau$ was assumed, where $f = \omega/2\pi$. The same scale was maintained for the other pictures which makes interpretation easier. To obtain the real scale of frequencies, the numbers found on the adopted scale should be divided by the time of propagation of the longitudinal, plane acoustic wave τ along the thickness of the piezoceramic element. The adopted value of the reflection coefficient $\beta_c = -0.9$ matches approximately the real conditions that are present on the boundary between the soft tissue and an average ceramics PZT.

The above transfer function shows resonance of thickness vibrations of the transducer that appear at $f\tau = 0.5$ and $f\tau = 1.5$. The resonance also appears periodically in higher frequencies with period $f\tau = 1$, while the values of the transfer function's module

decrease as $f\tau$ increases at pace $1/f\tau$. The use of the piezoceramic plate as a sensor of acoustic waves emitted by the temporomandibular joint should be tied to the frequency range which is below the first basic resonance. In this range, the transfer function's module is almost plane. The useful transmission band of the piezoceramic transducer is contained between the lower cut-off frequency f_m and upper cut-off frequency f_M. Figure 8 shows that half of the resonant frequency of the transducer can be adopted as the upper cut-off frequency.

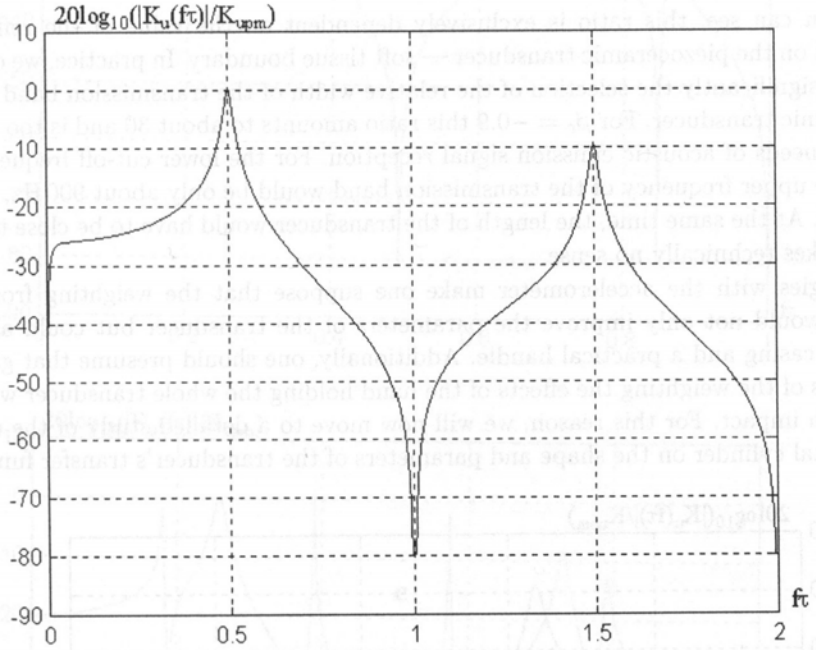

Fig. 8. Module of the shift function of the transducer without the metal cylinder: $\beta_b = 1$, $\tau_b/\tau = 0$, $K_{upm} = |K_u(0.5)|$, $\beta_c = -0.88$.

That's why, it is equal to approximately:

$$f_M = \frac{1}{4\tau} = \frac{c}{4d}. \tag{24}$$

The lower cut-off frequency can be determined from the transfer function (23) by using the approximation $\exp(-j\omega\tau) \cong 1 - j\omega\tau$, authorised for low frequencies. In this frequency range, the transfer function's module adopts the following form:

$$|K_u(j\omega)| = Y_3^D g_{33}\tau \cdot \frac{\omega\tau}{\sqrt{1+(\omega\tau)^2 A^2}}, \tag{25}$$

where

$$A = \frac{2\beta_c}{1+\beta_c}. \tag{26}$$

The lower cut-off frequency is determined from the condition $\omega_m \tau A = 2\pi f_m \tau A = 1$, and so:

$$f_m = \frac{1}{4\pi\tau} \frac{1+\beta_c}{\beta_c} = \frac{c}{4\pi d} \frac{1+\beta_c}{\beta_c}. \tag{27}$$

Equations (24) and (27) show that the relation between upper and lower cut-off frequency is approximately equal to:

$$\frac{f_M}{f_m} = \frac{\pi\beta_c}{1+\beta_c}. \tag{28}$$

As you can see, this ratio is exclusively dependent on the value of the reflection coefficient on the piezoceramic transducer — soft tissue boundary. In practice, we cannot influence significantly the selection of the relative width of the transmission band of the piezoceramic transducer. For $\beta_c = -0.9$ this ratio amounts to about 30 and is too low to meet the needs of acoustic emission signal reception. For the lower cut-off frequency of 30 Hz, the upper frequency of the transmission band would be only about 900 Hz, which is too low. At the same time, the length of the transducer would have to be close to 1 m, which makes technically no sense.

Analogies with the accelerometer make one suppose that the weighting from the backside would not only improve the parameters of the transducer but could also be used as a casing and a practical handle. Additionally, one should presume that given a large mass of the weighting the effects of the hand holding the whole transducer will not have much impact. For this reason, we will now move to a detailed study of the effects of the metal cylinder on the shape and parameters of the transducer's transfer function.

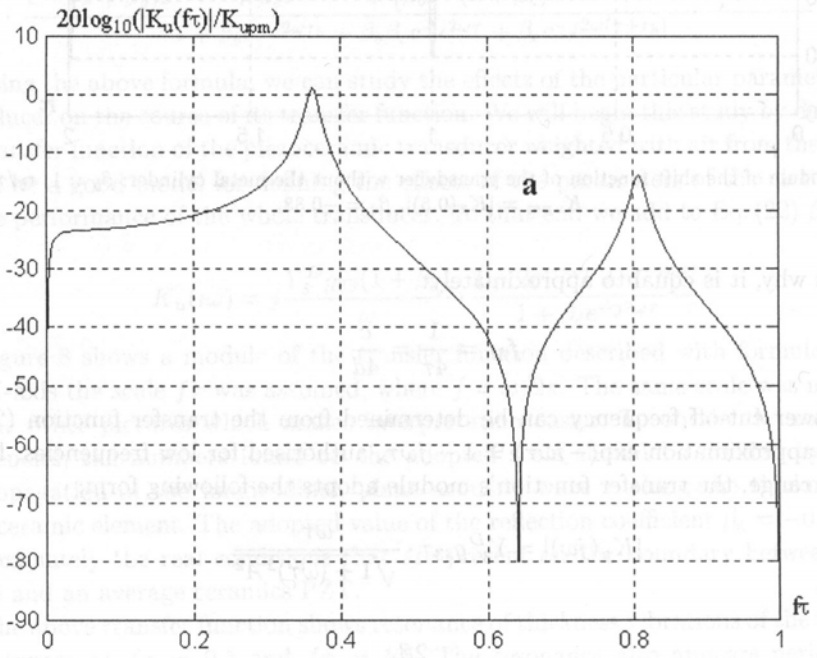

[FIG. 9 a]

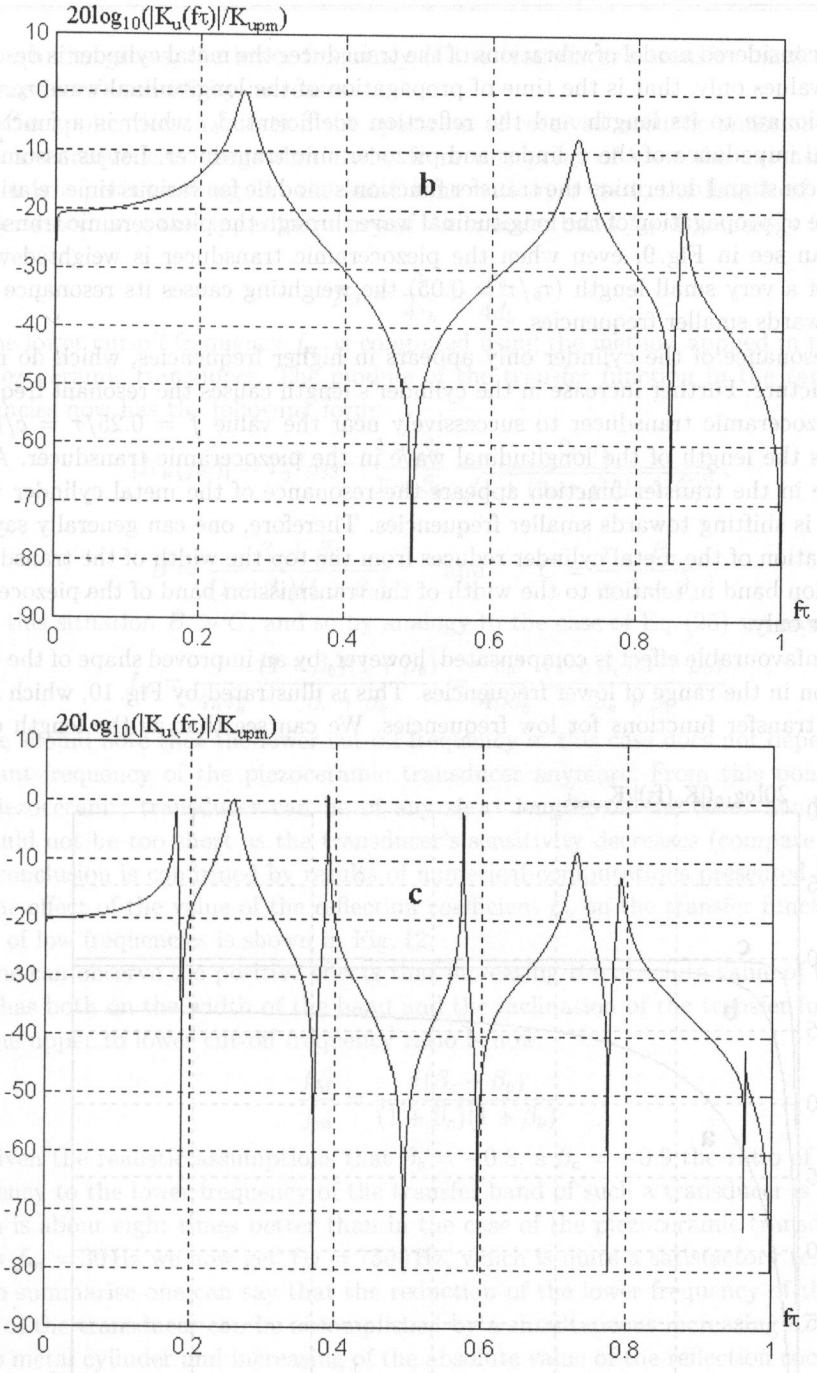

Fig. 9. The effects of the thickness of the cylinder on the module of the transducer's shift function ($\beta_b = -0.823$, $\beta_c = -0.88$, $K_{upm} = \max|Ku|$): a) $\tau_b/\tau = 0.05$, b) $\tau_b/\tau = 0.6$, c) $\tau_b/\tau = 2.6$.

In the considered model of vibrations of the transducer the metal cylinder is described with two values only, that is the time of propagation of the longitudinal wave τ_b, which is proportionate to its length and the reflection coefficient β_b, which is a function of mechanical impedance of the cylinder and piezoceramic transducer. Let us assume first that $\beta_b = \text{const}$ and determine the transfer function's module for various time relations τ_b to the time of propagation of the longitudinal wave through the piezoceramic transducer. As you can see in Fig. 9, even when the piezoceramic transducer is weighted with a cylinder of a very small length ($\tau_b/\tau = 0.05$) the weighting causes its resonance to be shifted towards smaller frequencies.

The resonance of the cylinder only appears in higher frequencies, which do not fit into the picture. Further increase in the cylinder's length causes the resonant frequency of the piezoceramic transducer to successively near the value $f = 0.25/\tau = c/(\lambda/4)$, where λ is the length of the longitudinal wave in the piezoceramic transducer. At the same time in the transfer function appears the resonance of the metal cylinder whose frequency is shifting towards smaller frequencies. Therefore, one can generally say that the application of the metal cylinder reduces from the top the width of the transducer's transmission band in relation to the width of the transmission band of the piezoceramic transducer only.

This unfavourable effect is compensated, however, by an improved shape of the transfer function in the range of lower frequencies. This is illustrated by Fig. 10, which shows the same transfer functions for low frequencies. We can see that as the length of the

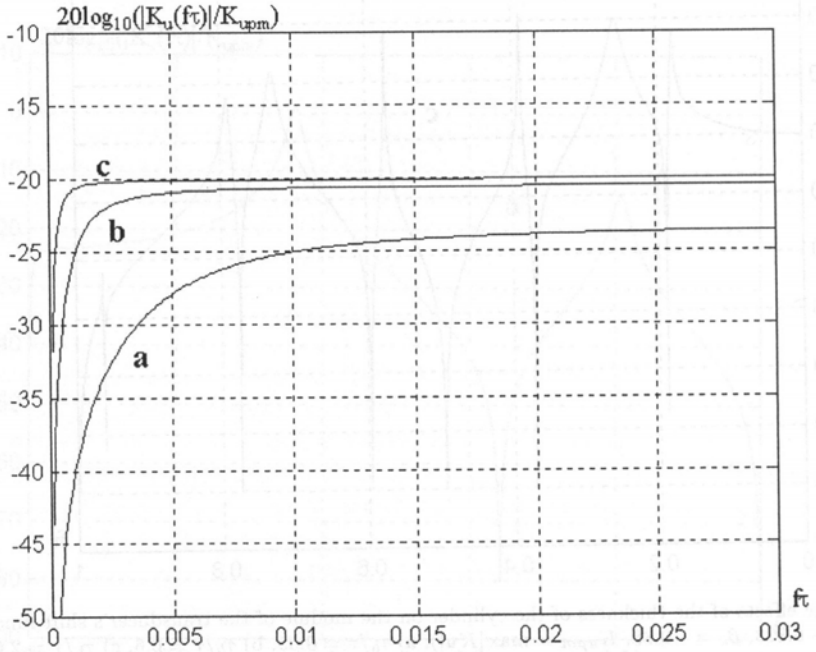

Fig. 10. Module of the transducer's shift function in the range of low frequencies ($\beta_b = -0.823$, $\beta_c = -0.88$, $K_{upm} = \max|K_u|$): a) $\tau_b/\tau = 0.05$, b) $\tau_b/\tau = 0.6$, c) $\tau_b/\tau = 2.6$.

metal cylinder grows, the lower frequency of the transducer's transfer band drops and the transducer's sensitivity increases.

In the application in question the spectrum of received acoustic emission signals is in the low frequencies range that's why from this point of view the extension of the cylinder is a positive thing. At the same time with $\tau_b/\tau \gg 1$, the length of the metal cylinder determines the upper frequency of the transfer band f_M. By analogy to Eq. (24) we have:

$$f_M = \frac{1}{4\tau_b} = \frac{c_b}{4d_b}. \tag{29}$$

The lower cut-off frequency f_m is computed using the method applied in the case of the piezoceramic transducer. The module of the transfer function in the range of low frequencies now has the following form:

$$|K_u(j\omega)| = Y_3^D g_{33}\tau \cdot \frac{1-\beta_b}{1+\beta_b} \frac{2\omega\tau_b}{\sqrt{1+(2\omega\tau_b)^2(B+C)^2}}, \tag{30}$$

where

$$B = \frac{\beta_c+\beta_b}{(1+\beta_c)(1+\beta_b)} \qquad \text{and} \qquad C = \frac{\tau}{\tau_b}\frac{\beta_c}{1+\beta_c}. \tag{31}$$

In this situation $B \gg C$, and so by analogy to the case of Eq. (25) we have:

$$f_m = \frac{1}{4\pi\tau_b}\frac{(1+\beta_c)(1+\beta_b)}{\beta_c+\beta_b} = \frac{c_b}{4\pi d_b}\frac{(1+\beta_c)(1+\beta_b)}{\beta_c+\beta_b}. \tag{32}$$

We should note that the lower cut-off frequency in this case does not depend on the resonant frequency of the piezoceramic transducer anymore. From this point of view the piezoceramic transducer can be of any short length, on the other hand however, it should not be too short as the transducer's sensitivity decreases (compare Eq. (30)). This conclusion is confirmed by results of numerical computations presented in Fig. 11.

The effect of the value of the reflection coefficient β_b on the transfer function in the range of low frequencies is shown in Fig. 12.

One can observe the positive effects that increasing the absolute value of this coefficient has both on the width of the band and the inclination of the transfer function.

The upper to lower cut-off frequency ratio is now:

$$\frac{f_M}{f_m} = \frac{\pi(\beta_c+\beta_b)}{(1+\beta_c)(1+\beta_b)}. \tag{33}$$

Given the realistic assumptions that $\beta_b = -0.8$, a $\beta_c = -0.9$ the ratio of the upper frequency to the lower frequency of the transfer band of such a transducer is about 250 which is about eight times better than in the case of the piezoceramic transducer only. Given $f_m = 30\,\text{Hz}$ we now get $f_M = 7500\,\text{Hz}$, which is quite a satisfactory result.

To summarise one can say that the reduction of the lower frequency of the transfer band of the transducer can be accomplished by a simultaneous increasing of the length of the metal cylinder and increasing of the absolute value of the reflection coefficient β_b. If the metal cylinder is made of a material of a specific acoustic impedance $\rho_b c_b$, the value of the reflection coefficient increases parallel to the increase in the surface of the cylinder's base. As a result, the combined increase in the cylinder's length and reflection coefficient is in this case equivalent to the increase in its mass.

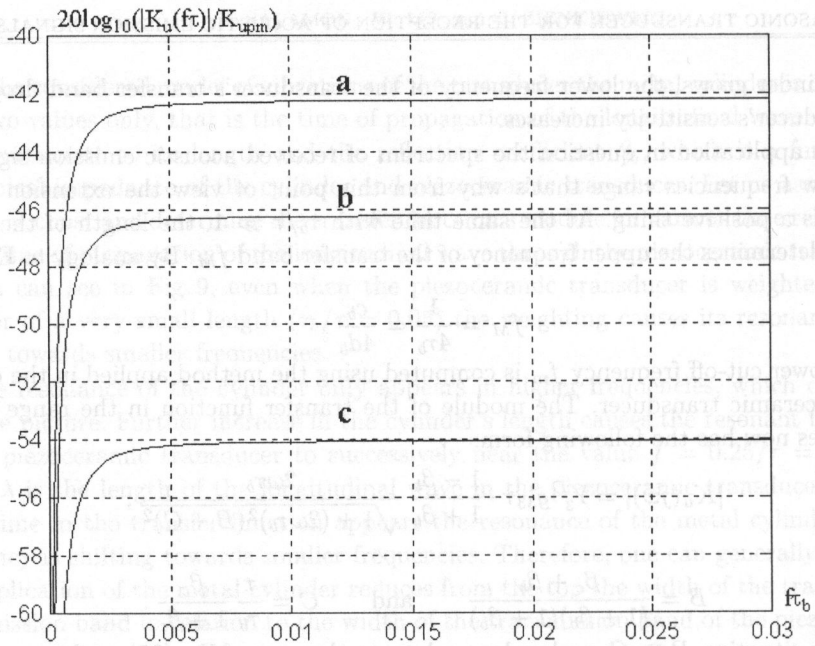

Fig. 11. Module of the transducer's shift function given a constant length of the metal cylinder — low frequencies range ($\beta_b = -0.823$, $\beta_c = -0.88$, $K_{upm} = \max|K_u|$): a) $\tau/\tau_b = 0.8$, b) $\tau/\tau_b = 0.5$, c) $\tau/\tau_b = 0.2$.

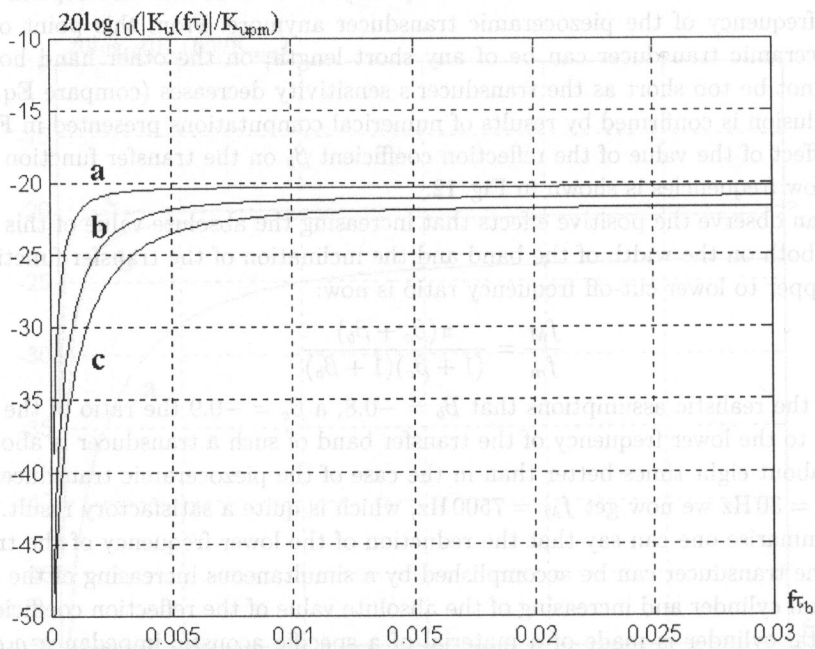

Fig. 12. The effects of the diameter of the metal cylinder on the module of the transducer's shift function within low frequencies range ($\beta_c = -0.88$, $\tau_b/\tau = 0.6$, $K_{upm} = \max|K_u|$): a) $\beta_b = -0.9$, b) $\beta_b = -0.7$, c) $\beta_b = -0.5$.

5. Design, construction and measurements of the transducer

The transducer was designed and later built on the basis of the following operating assumptions:

- effective transfer band of the transducer should be between app.10 Hz to about 10 kHz, which ensures a transfer without distortion of acoustic emission signals,
- considering the convenience of using the transducer its total length should not exceed 15 cm, with total mass less than 1 kg and diameter of the metal cylinder not to exceed 4 cm,
- the ratio of the surface of the metal cylinder to the surface of the piezoceramic transducer should not be greater than 10 which reduces the effects of transverse vibrations of the metal cylinder on the transducer's transfer function, [5].

Since the mass of the metal cylinder should be big, it was decided to make it of brass of density of $\rho_b = 8100\,\mathrm{kg/m^3}$. Elementary computations show that given the admissible mass and diameter of the cylinder, its length should not exceed 10 cm. By adding to Eq. (29) $d_b = 0.1\,\mathrm{m}$ and the velocity of the longitudinal wave in brass equal to approximately $c_b = 4000\,\mathrm{m/s}$ we get $f_M = 10\,\mathrm{kHz}$. This frequency is equal to the upper frequency of the required transfer band of the transducer.

By making the preliminary assumption that the lower cut-off frequency of the transducer $f_m = 10\,\mathrm{Hz}$ and that the reflection coefficient on the transducer-body boundary is equal to $\beta_c = -0.88$, from Eq. (33) we denote $\beta_b = -0.95$. Given this value of the reflection coefficient the ratio of the mechanical impedance of the brass cylinder Z_b to the mechanical impedance of the piezoceramic transducer would have to be 39. Given the similar values of acoustic impedance of both materials this would require a significant differentiation between the surface of the cylinder and the piezoceramic transducer. Because it is contrary to the above criterion, we are forced to abandon the assumption that $f_m = 10\,\mathrm{Hz}$. And so we are increasing the lower cut-off frequency to $f_m = 40\,\mathrm{Hz}$ and from Eq. (33) we denote the value of the reflection coefficient $\beta_b = -0.823$. As a result, the ratio Z_b/Z is now 10.3 and is acceptable.

If we assume that the radius of the surface of the metal cylinder is $r = 2\,\mathrm{cm}$ we compute the mechanical impedance $Z_b = \pi r^2 \rho_b$, $c_b = 40694\,\mathrm{kg/s}$ and mechanical impedance of the piezoceramic transducer $Z = Z_b/10.3 = 3951\,\mathrm{kg/s}$. The applied transducer is made of PZT ceramics of density $\rho = 7030\,\mathrm{kg/m^3}$, and velocity $c = 3480\,\mathrm{m/s}$. From the equation $A = Z/\rho c$ we compute the field of the surface of the piezoceramic transducer $A = 1.61\,\mathrm{cm^2}$.

The last value we are looking for is the length of the piezoceramic transducer d. It should be long enough for the transducer's resonant frequency to be higher than the resonant frequency of the metal cylinder which in this case is in excess of 20 kHz. The selected transducer's resonant frequency is 60 kHz with no acoustic weighting which is a frequency of $f_r = 30\,\mathrm{kHz}$ when weighted with a brass cylinder. The length of the transducer is $d = c/4f_4 = 2.9\,\mathrm{cm}$.

The theoretical transfer function in this design of the transducer denoted from Eq. (22) is shown in Fig. 13.

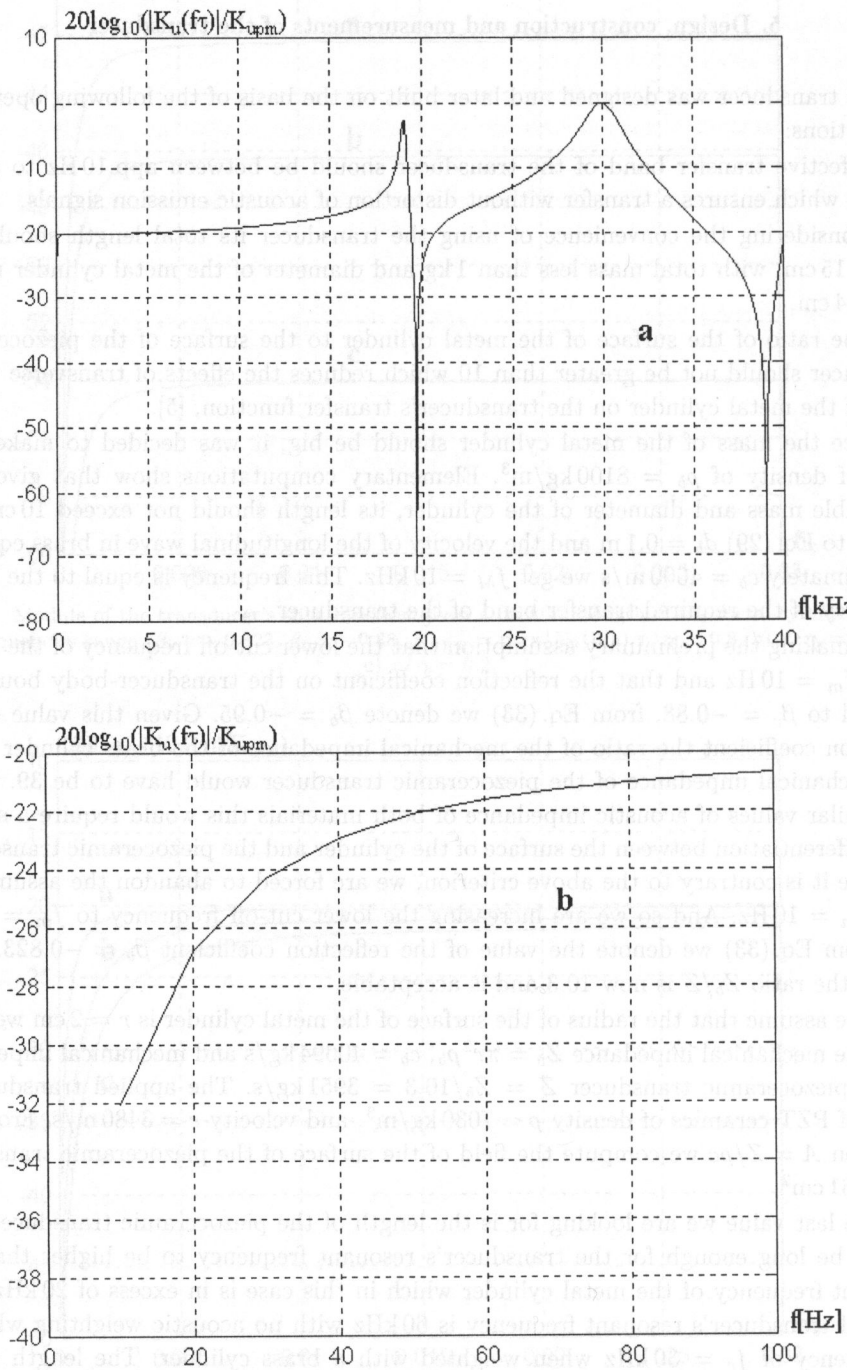

Fig. 13. Module of the shift function of the designed transducer.

As you can see, the location of the resonance meets the expectations. What is more important the transfer band in the low frequency range is almost plane up to frequency 40 Hz. Attenuation in this frequency is as little as 3 dB in relation to attenuation in the transfer band. At frequency of 10 Hz, the sensitivity of the transducer is smaller by 9 dB. Therefore, it is safe to say that the designed transducer transfers acoustic emission signals without significant distortion in the band from 40 Hz to 10 kHz. Attenuation of signals in the band from 10 Hz to 40 Hz is sufficiently small and does not exclude observation of the signals in this band.

The transducer was built based on the above design. Its construction is shown in Fig. 14.

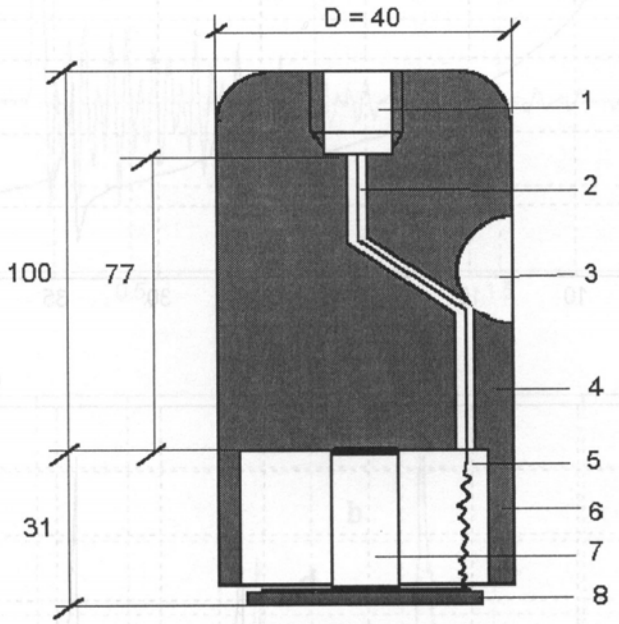

Fig. 14. The structure of the transducer — axial alignment: 1 – opening for the signal socket, 2 – duct for electrical wire, 3 – technological opening, 4 – brazen body (cylinder), 5 – niche, 6 – shielding of the ceramics, 7 – piezoelectric transducer, 8 – shielding and the active electrode.

To verify the theoretical and design computations its electrical impedance was measured $Z_e(f)$. The module of the impedance multiplied by the frequency should, according to the theory, describe the transducer's transfer function, [5, 13]. As is shown in Fig. 15 the transfer function of the transducer built is similar to the theoretical transfer function shown in Fig. 13.

The only variances apply to the placement of the resonance of the metal cylinder and the appearance of an additional resonance at the frequency of about 17 kHz. The increase in the resonant frequency of the brass cylinder is the result of the opening (1) lying opposite the piezoceramic transducer. The path between the bottom of the opening and the surface of the transducer is $d_b' = 77\,\text{mm}$ which at velocity of $c_b = 4000\,\text{m/s}$ gives the resonance frequency of 26 kHz. Lack of resonance at frequency of 20 kHz can

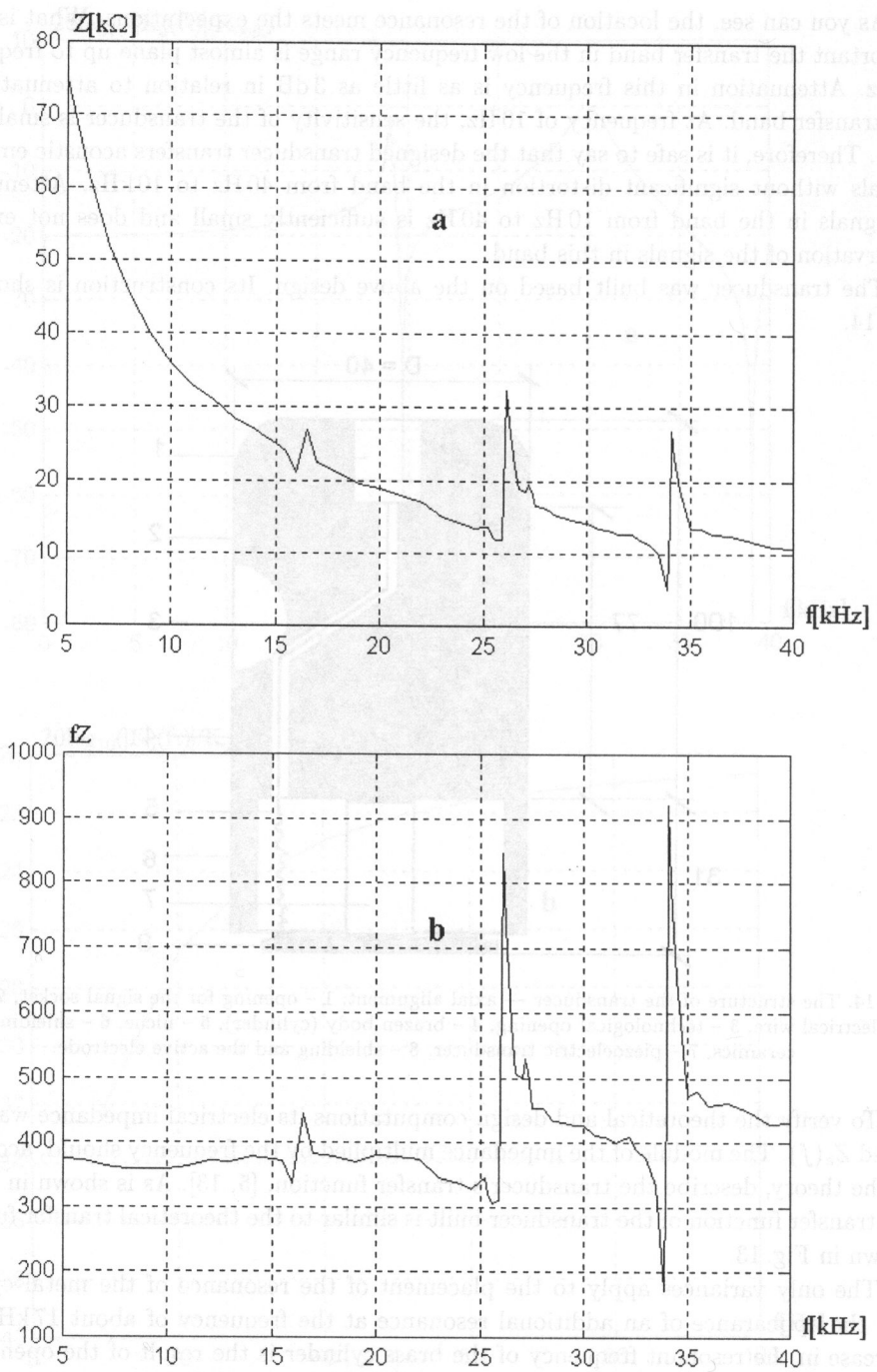

Fig. 15. Electric impedance of the transducer: a) module of electric impedance, b) product of the module of electric impedance and the frequency.

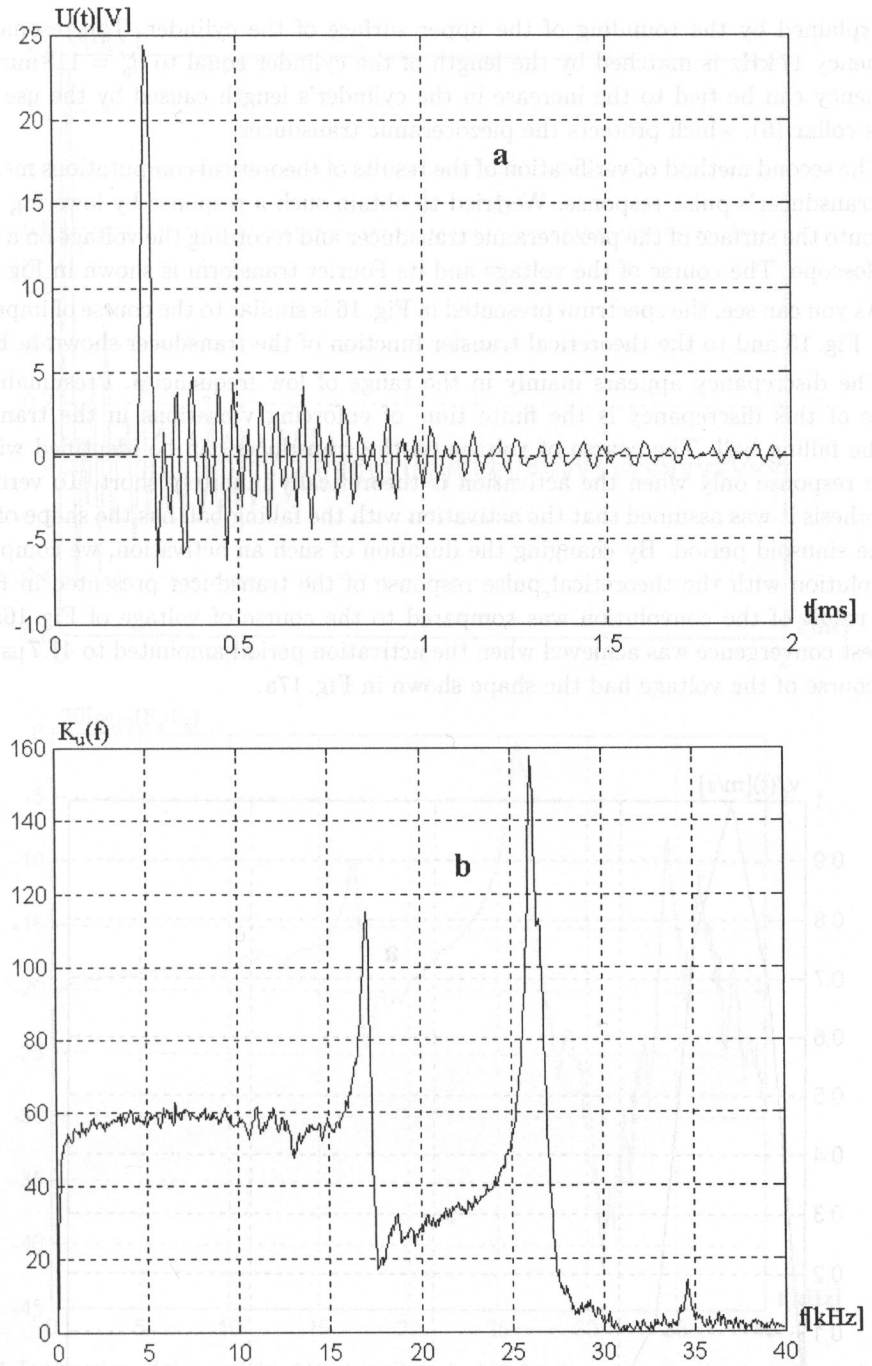

Fig. 16. Voltage response of transducer as it is hit with a metal ball a) transducer's response in time, b) module of the spectrum of the transducer's response.

be explained by the rounding of the upper surface of the cylinder. The resonance at frequency 17 kHz is matched by the length of the cylinder equal to $d_b'' = 118$ mm. This frequency can be tied to the increase in the cylinder's length caused by the use of the brass collar (6), which protects the piezoceramic transducer.

The second method of verification of the results of theoretical computations measured the transducer's pulse response. We tried to obtain such a response by lowering a steel ball onto the surface of the piezoceramic transducer and recording the voltage on a digital oscilloscope. The course of the voltage and its Fourier transform is shown in Fig. 16.

As you can see, the spectrum presented in Fig. 16 is similar to the course of impedance from Fig. 15 and to the theoretical transfer function of the transducer shown in Fig. 13.

The discrepancy appears mainly in the range of low frequencies. Presumably, the cause of this discrepancy is the finite time of enforcing vibrations in the transducer by the falling ball. The course of voltage on the transducer can be identified with the pulse response only when the activation is theoretically infinitely short. To verify this hypothesis it was assumed that the activation with the falling ball has the shape of a half of the sinusoid period. By changing the duration of such an activation, we compute its convolution with the theoretical pulse response of the transducer presented in Fig. 7a. The result of the convolution was compared to the course of voltage of Fig. 16a. The highest convergence was achieved when the activation period amounted to 41.7 μs. Then the course of the voltage had the shape shown in Fig. 17a.

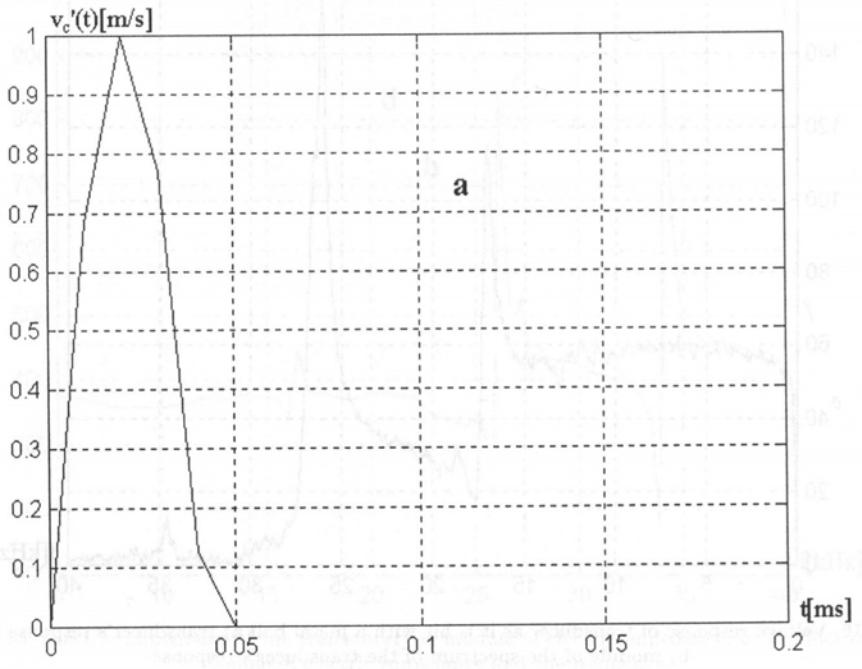

[FIG. 17a]

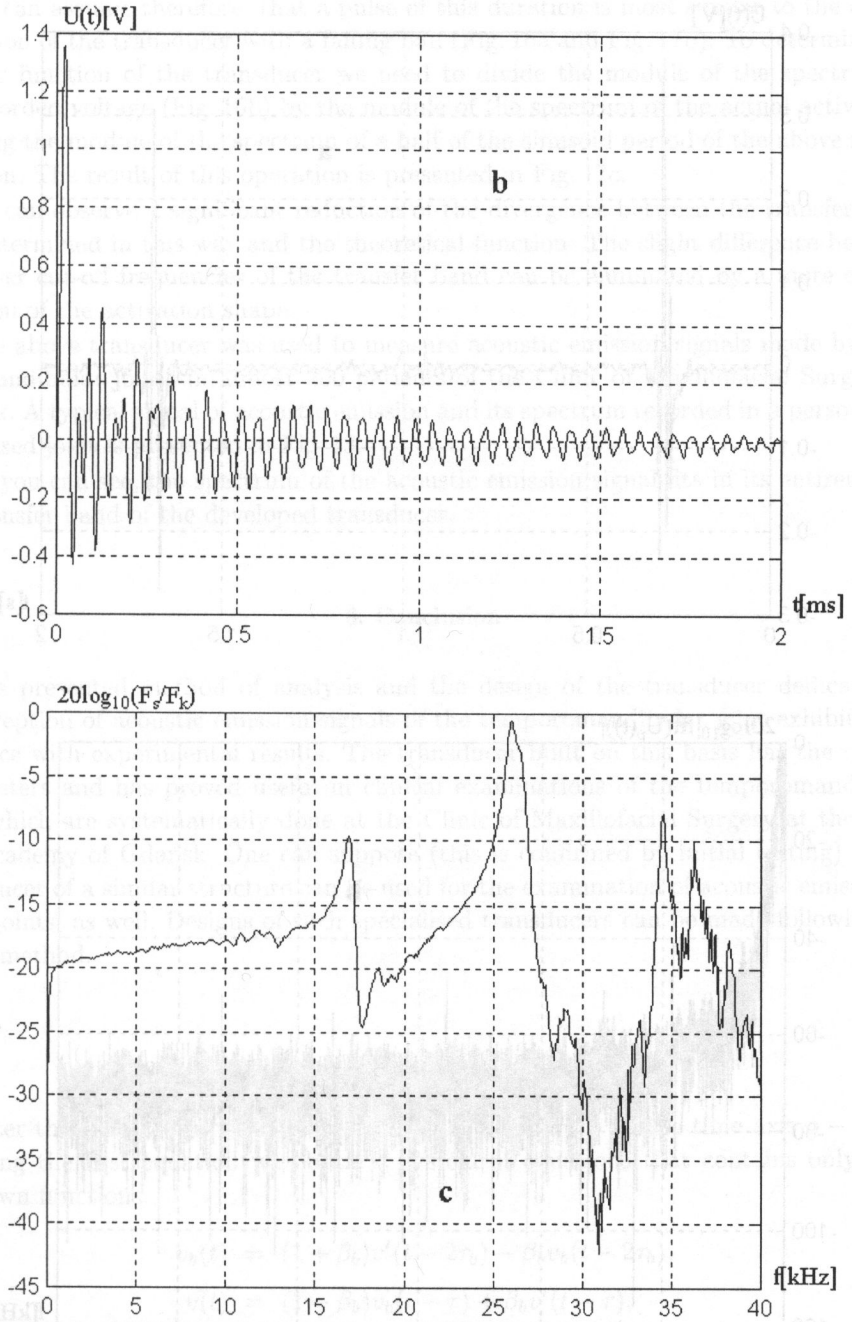

Fig. 17. Designation of the module of the transducer's shift function: a) activation imitating a falling ball, b) transducer's response — a convolution of the pulse response (Fig. 7 a) with the activation that imitates a falling ball, c) module of the shift function computed as the relation between the modules of the signal's spectra from Fig. 17 a and the module of the spectrum of the signal imitating the activation with the ball (half of the sinusoid).

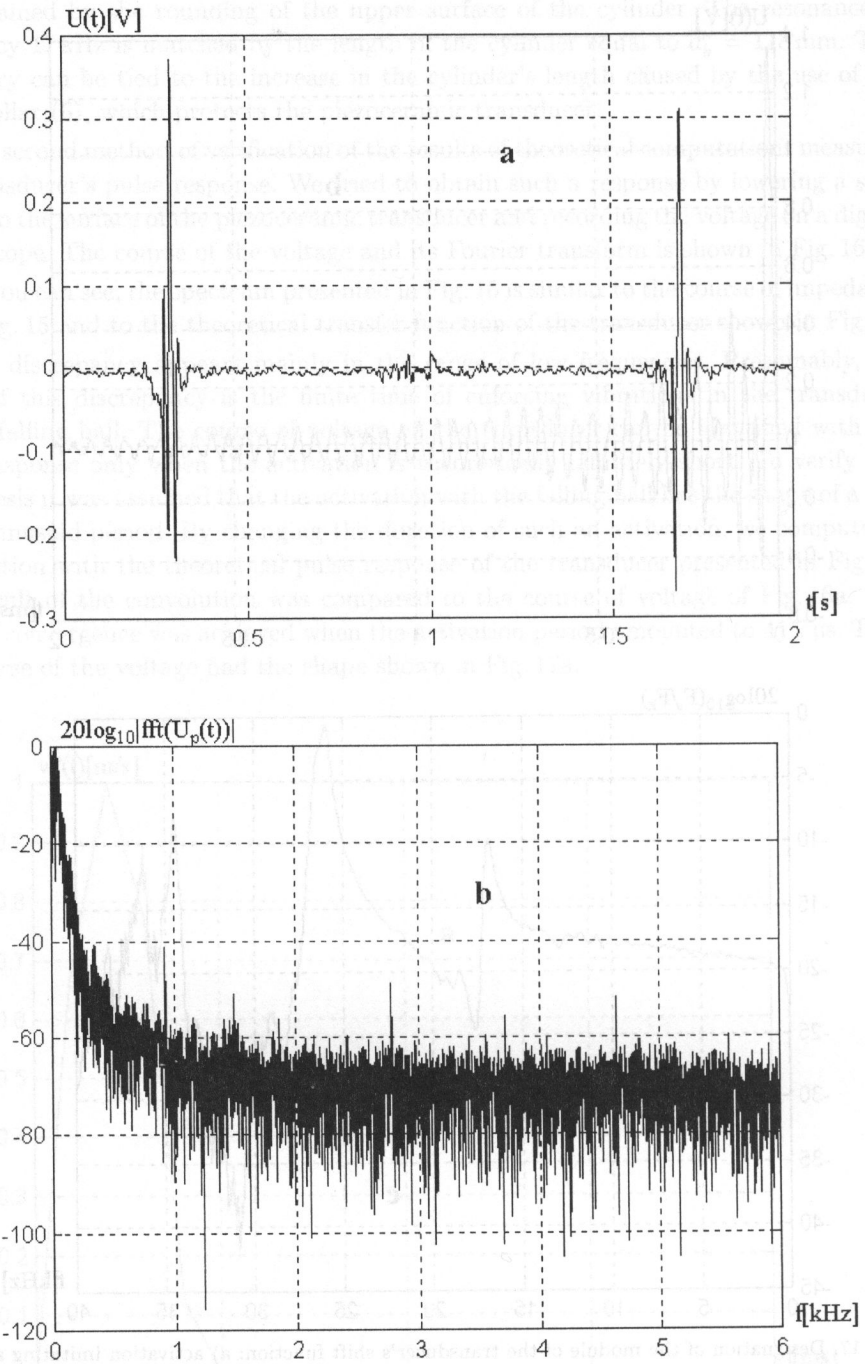

Fig. 18. A typical acoustic signal recorded in a patient: a) the time course, b) signal's spectrum.

We can assume therefore, that a pulse of this duration is most similar to the actual activation of the transducer with a falling ball (Fig. 16a and Fig. 17b). To determine the transfer function of the transducer we need to divide the module of the spectrum of the recorded voltage (Fig. 16b) by the module of the spectrum of the actual activation, meaning the module of the spectrum of a half of the sinusoid period of the above stated duration. The result of this operation is presented in Fig. 17c.

We can observe a significant reduction of the divergence between the transfer function determined in this way and the theoretical function. The slight difference between the lower cut-off frequencies of the transfer band can be eliminated by a more careful selection of the activation shape.

The above transducer was used to measure acoustic emission signals made by temporomandibular joints in almost 200 patients of the Clinic of Maxillofacial Surgery in Gdańsk. A typical signal of acoustic emission and its spectrum recorded in a person with a diseased joint is presented in Fig. 18.

As you can see, the spectrum of the acoustic emission signal fits in its entirety into the transfer band of the developed transducer.

6. Conclusion

The presented method of analysis and the design of the transducer dedicated to the reception of acoustic emission signals of the temporomandibular joint exhibits convergence with experimental results. The transducer built on this basis has the desired parameters and has proved useful in clinical examinations of the temporomandibular joint which are systematically done at the Clinic of Maxillofacial Surgery at the Medical Academy of Gdańsk. One can suppose (this is confirmed by initial testing) that a transducer of a similar structure can be used for the examination of acoustic emission of other joints, as well. Designs of such specialised transducers can be made following the above method.

Appendix

After the shift of functions that are present in Eq. $(4)_2$ on the time axis $o - \tau_b$ and inserting the first equation we obtain a system of equations that contains only three unknown functions.

$$\begin{aligned} v_b(t) &= (1+\beta_b)v'(t-2\tau_b) - \beta_b v_b(t-2\tau_b), \\ v(t) &= (1-\beta_b)v_b(t-\tau) + \beta_b v'(t-\tau), \\ v'(t) &= (1+\beta_c)v'_c(t-\tau) - \beta_c v(t-\tau). \end{aligned} \tag{A.1}$$

To further reduce the number of unknown functions we can eliminate velocity $v'(t)$. To that end we multiply the first equation by β_b and shift $o-\tau$, and multiply the second

equation by $(1+\beta_b)$ and shift $o-2\tau_b$. We then get:

$$\begin{aligned} \beta_b v_b(t-\tau) &= \beta_b(1+\beta_b)v'(t-2\tau_b-\tau) - \beta_b^2 v_b(t-2\tau_b-\tau), \\ (1+\beta_b)v(t-2\tau_b) &= (1-\beta_b^2)v_b(t-\tau-2\tau_b) + \beta_b(1+\beta_b)v'(t-\tau-2\tau_b). \end{aligned} \tag{A.2}$$

After subtracting the above equations by the sides and arranging the expressions we get:

$$\beta_b v_b(t-\tau) + v_b(t-\tau-2\tau_b) = (1+\beta_b)v(t-2\tau_b), \tag{A.3}$$

By applying the same operations to the first and third equation from the system of equations (A.1) we have:

$$v_b(t) + \beta_b v_b(t-2\tau_b) = (1+\beta_b)\Big[-\beta_c v(t-\tau-2\tau_b) + (1+\beta_c)v_c'(t-\tau-2\tau_b)\Big]. \tag{A.4}$$

Equations (A.3) and (A.4) contain two unknown functions, that is $v_b(t)$ and $v(t)$. Let us now multiply the equation (A.3) by β_c and shift $o-\tau$. This gives us:

$$\beta_c\beta_b v_b(t-2\tau) + \beta_c v_b(t-2\tau-2\tau_b) = (1+\beta_b)\beta_c v(t-\tau-2\tau_b). \tag{A.5}$$

After adding by the sides the equations (A.4) and (A.5) we get:

$$\begin{aligned} v_b(t) + \beta_b v_b(t-2\tau_b) + \beta_b\beta_c v_b(t-2\tau) + \beta_c v_b(t-2\tau_b-2\tau) \\ = (1+\beta_b)(1+\beta_c)v_c'(t-\tau-2\tau_b). \end{aligned} \tag{A.6}$$

Equation (A.6) is a non-homogenous difference equation with continuous time of the function $v_b(t)$. On the right side of the equation is as usual the activation — in our case it is velocity $v_c'(t)$. To simplify the notation of further equations let us introduce the following notation:

$$r(t) = \delta(t) + \beta_b\delta(t-2\tau_b) + \beta_b\beta_c\delta(t-2\tau) + \beta_c\delta(t-2\tau-2\tau_b), \tag{A.7}$$

where $\delta(t)$ is Dirac's distribution.

Using the above notation, the difference equation (A.6) can be written as:

$$v_b(t) * r(t) = (1+\beta_b)(1+\beta_c)v_c'(t-\tau-2\tau_b), \tag{A.8}$$

where symbol (*) means the convolution operation.

Let us now denote equations which describe the other wanted functions, that is velocities $v(t)$ and $v'(t)$. To that end, let us note the first of the equations (A.1) in the form of a convolution with the function $r(t)$:

$$v_b(t) * r(t) + \beta_b v_b(t-2\tau_b) * r(t) = (1+\beta_b)v'(t-2\tau_b) * r(t). \tag{A.9}$$

Next using the equation (A.8), we have:

$$(1+\beta_b)(1+\beta_c)\Big[v_c'(t-\tau-2\tau_b) + \beta_b v_c'(t-\tau-4\tau_b)\Big] = (1+\beta_b)v'(t-2\tau_b) * r(t). \tag{A.10}$$

After simplifications, the above equation assumes the following form:

$$v'(t) * r(t) = (1+\beta_c)\Big[v_c'(t-\tau) + \beta_b v_c'(t-\tau-2\tau_b)\Big]. \tag{A.11}$$

Similarly, the difference equation is obtained in relation to velocity $v(t)$:

$$v(t) * r(t) = (1-\beta_b)v_b(t-\tau) * r(t) + \beta_b v'(t-\tau) * r(t). \tag{A.12}$$

Equations (A.8), (A.11) and (A.12) are used in the main text of the article.

Acknowledgements

The authors wish to express their gratitude to Professor Tadeusz Korzon, at the time the head of the Department and the Clinic of Maxillofacial Surgery at the Medical Academy in Gdańsk for having initiated the acoustic examination of the temporomandibular joint, for the many years of support for the studies and for the inspiring discussions on the directions and methods of the studies. We wish to thank Professor Leszek Filipczyński — full member of the Polish Academy of Sciences and Andrzej Stepnowski from the Department of Acoustics of the Technical University of Gdańsk for the valuable comments on the theory and measurements of the transducer.

References

[1] R. BADWAL, *The application of fractal dimension to temporomandibular joint sounds*, Comput. Biol. Med., **23**, 1, 1–14 (1993).

[2] L.V. CHRISTENSEN, *Physics and the sounds produced by the temporomandibular joints*, Journal of Oral Rehabilitation, **19**, Part I. 471–483, Part II. 615–627 (1992).

[3] R. DOVE, R. FRIGHT, B. PRICE, K. SCALLY and R. TREMEWAN, *Tracking jaw movement*, Medical & Biological Engineeering & Computing, September 32, 584–588 (1994).

[4] R. DRUM and M. LITT, *Spectral analysis of temporomandibular joint sounds*, The Journal of Prosthetic Dentistry, **58**, 4, 485–494 (1987).

[5] L. FILIPCZYŃSKI, *Transients and the equivalent electrical circuit of piezoelectric transducer*, Acustica, **10**, 149–154 (1960).

[6] T. GAY and C.N. BERTOLAMI, *The spectral properties of temporomandibular sounds*, J. Dent., Res., **66**, 6, 1189–1194 (1987).

[7] L. HEFFEZ and D. BLAUSTEIN, *Advances in sonography of the temporomandibular joint*, Oral Surg. Oral Med. Oral Pathol., **62**, 486–495 (1986).

[8] H.W. KATZ, *Solid state magnetic and dielectric devices*, John Wiley & Sons, Inc., New York 1959, 120.

[9] J. KRASZEWSKI and Z. KRASZEWSKA, *Phonoarthographic diagnostics of temporomandibular joint* [in Polish], Czas. Stomat., **28**, 3, 279–285 (1975).

[10] J. KRASZEWSKI and Z. KRASZEWSKA, *Phonoarthographic diagnostic in certain temporomandibular joint dysfunction* [in Polish], Czas. Stomat., **28**, 4, 387–396 (1975).

[11] W. LIS, J. ZIENKIEWICZ and R. SALAMON, *Parameters of acoustic signal emitted by the temporomandibular joint* [in Polish], Proceedings XLIII OSA, Gliwice – Ustroń, 457–462 (1996).

[12] W. LIS and J. ZIENKIEWICZ, *The wavelet transform analysis of the temporomandibular joint acoustic emission* [in Polish], Proceedings XLIV OSA, Gdańsk – Jastrzębia Góra, 423–428 (1997).

[13] G. ŁYPACEWICZ and E. DURIASZ, *Compensating circuit of ultrasonic probe* [in Polish], Proceedings X Symposium on Hydroacoustics, Jurata May, 139–144 (1993).

[14] G. ŁYPACEWICZ, *Design of ultrasonic probes for medical diagnostics* [in Polish], Proceedings IX Symposium on Hydroacoustics, Gdynia – Jurata, 11–30 (1992).

[15] A. MARKIEWICZ and G. ŁYPACEWICZ, *Application of matching layers of ultrasonic probes to biological structures* [in Polish], Prace OSA XXI, Rzeszów, 139–141 (1974).

[16] C. OSTER, R.W. KATZBERG, R.H. TALLENTS, T.W. MORRIS, J. BARTHOLOMEW, T.L. MILLER and K. HAYAKAWA, *Characterization of temporomondibular joint sounds*, Oral Surg., **58**, 10–16 (1984).

[17] R. SALAMON, *Wellenmodell des Beschleunigunsmessers*, Fortschritte der Akustik Duisburg DAGA, 275–278 (1989).

[18] R. SALAMON and F. CHINCHURRETA, *Signalmodell des piezoelektrischen Schwingers*, Acustica, **66**, 247–257 (1988).

[19] R. SALAMON and F. CHINCHURRETA, *Analyse piezoelektrischer Breitbandschwinger mit Differenzengleichung*, Acustica, **67**, 19–29 (1988).

[20] D.M. WATT, *Clinical applications of gnathosonics*, Prosthetic Department, School of Dental Surgery, University of Edinburgh, Scotland, I-II, 16, 83–95 (1966).

[21] R.M. WILK and S.E. HARMS, *Temporomandibular joint: Multislab, threee-dimensional Fourier transformation MR imaging*, Radiology, **167**, 3, 861–863 (1988).

[22] I. YAVELOW and G.S. ARNOLD, *Temporomondibular joint clicking*, Oral Surg., **32**, 708–714 (1971).